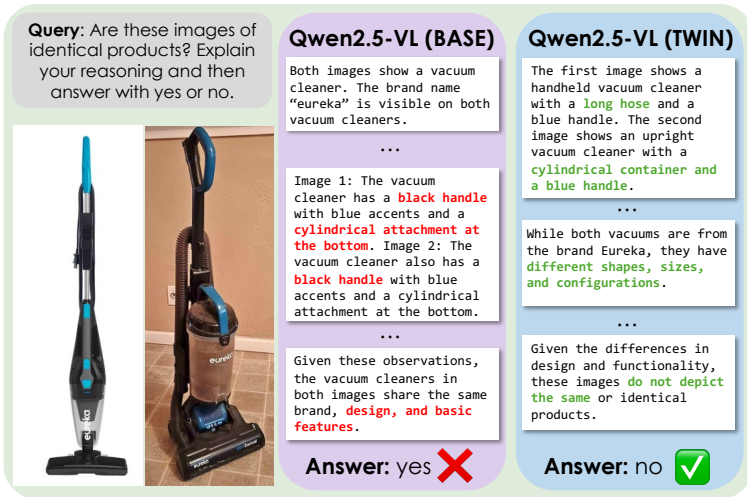
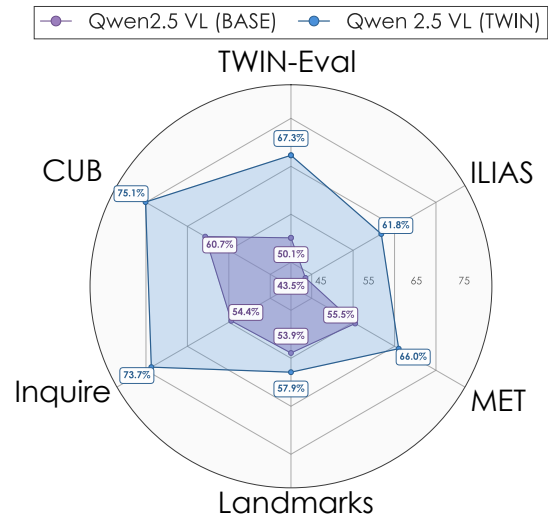


Same or Not? Enhancing Visual Perception in Vision-Language Models

Damiano Marsili Aditya Mehta Ryan Y. Lin Georgia Gkioxari
 California Institute of Technology



(a) The TWIN Dataset



(b) The FGVQA Benchmark Suite

Figure 1. (a) Fine-grained visual understanding requires recognizing subtle differences between similar images. We introduce TWIN, a large-scale dataset of 561K image-pair queries asking if two images depict the same object, and FGVQA, a benchmark suite evaluating fine-grained VQA capabilities. (b) Models trained on TWIN show improved fine-grained understanding on FGVQA, even in unseen domains.

Abstract

Vision-language models (VLMs) excel at broad visual understanding but remain coarse-grained, exhibit visual biases, and miss subtle visual details. Existing training corpora reinforce this limitation by emphasizing general recognition (“Is it a cat or a dog?”) over fine-grained perception. To address this, we introduce a new training corpus and task designed to enhance the perceptual abilities of VLMs. TWIN is a large-scale dataset of 561,000 image-pair queries that task models to determine whether two visually similar images depict the same object, encouraging attention to nuanced visual cues. The dataset spans a diverse range of everyday objects across contexts, viewpoints, and appearances. Fine-tuning VLMs on TWIN yields notable gains in fine-grained recognition, even on unseen domains such as art, animals, plants, and landmarks. To quantify these gains, we introduce FGVQA, a benchmark suite of 12,000 queries that repurposes fine-grained recognition and retrieval datasets from multiple domains. While existing VLMs struggle on FGVQA, when fine-tuned on TWIN they improve by up to 19.3%, without compromising per-

formance on general VQA benchmarks. Finally, our TWIN dataset scales favorably with object annotations, and our analysis shows that scale is key to performance. We envision TWIN as a drop-in addition to open-source VLM training corpora, advancing perceptual precision of future models. Project webpage: <https://glab-caltech.github.io/twin/>

1. Introduction

Fine-grained visual understanding – recognizing subtle details within images – is a hallmark of human vision and a desirable goal for machine perception. Modern vision-language models (VLMs) have shown tremendous progress in broad visual reasoning, however their perception remains coarse-grained: they exhibit systematic biases [38, 74, 89, 90] and overlook subtle details [19, 69]. Fig. 1(a) showcases these challenges. While the vacuum cleaners share the same color and brand name, they are distinct instances, distinguishable by the geometry of their dustbins, handle, and base. Qwen2.5-VL [5], a strong open-source VLM, incorrectly identifies them as identical and reveals flawed reasoning about their visual attributes.

We attribute the limitations of current VLMs in fine-grained perception partly to their training data. Most large-scale image–text corpora emphasize general visual reasoning – such as spatial relations [27, 30, 53, 83], common knowledge [51, 108], grounding [31, 36, 66, 85, 110], or mathematical reasoning [3, 48, 93, 112] – over detailed visual discrimination. While these datasets enable broad understanding, they provide little incentive to attend to subtle, instance-level differences. This imbalance is stark in leading open-data VLMs [10, 50], where the majority of their training data does not reward visual distinctions beyond category-level understanding.

We ask: what if VLMs were trained on data that rewards fine-grained visual understanding? To explore this question, we introduce TWIN, a large-scale VQA dataset of 561,000 instance-centric queries. We name our dataset TWIN as it features TTwo-image INstance comparisons: each query asks whether two images depict the same physical object instance, requiring attention to subtle visual cues beyond category-level semantics. We source images of household objects across diverse backgrounds, viewpoints, contexts, and lighting conditions, verified by human annotators. We focus on household objects as their images are readily available and they are central to common visual tasks such as robotics and embodied interaction. Fig. 1(a) shows a sample from TWIN and illustrates the challenge: distinguishing the vacuum cleaners requires noting differences in form factor and shape, rather than shared brand or color.

To evaluate progress in fine-grained visual perception in VLMs, we introduce FGVQA, a benchmark suite for fine-grained VQA. While fine-grained recognition tasks have long existed in vision research, they are typically formulated as 1-of-N classification or retrieval problems, making them ill-suited for VLMs. FGVQA adapts and reformulates existing recognition and retrieval datasets for VLM evaluation, comprising 12,000 queries from diverse domains: MET [107] with artworks such as paintings and sculptures, INQUIRE [88] featuring animals and plants from iNaturalist [87], CUB [91] with bird species, ILIAS [33] showcasing retail products, and LANDMARKS [97] containing landmarks such as monuments and architectural structures.

VLMs post-trained on TWIN show substantial gains on FGVQA, as illustrated in Fig. 1(b) which compares the base and post-trained Qwen2.5-VL. Notably, the gains are substantial even on domains that span beyond TWIN, *e.g.* in INQUIRE and CUB. Through qualitative analyses of model explanations and probing experiments on the vision encoder, we find that VLMs trained on TWIN attend more effectively to nuanced, distinguishing visual cues. Finally, our scaling analysis shows that scale is crucial for performance, establishing TWIN, which scales in size favorably with the number of object annotations, as a promising path for advancing perceptual precision in VLMs.

2. Related Work

Limitations of VLMs. VLMs trained on large text-image corpora have shown remarkable capabilities in image understanding. Here, proprietary systems [1, 4, 13, 63] lead in performance, while open-source alternatives [15, 16, 43, 50, 55, 81, 99] are narrowing the gap. Despite these advances, VLMs exhibit systematic biases [38, 74, 89, 90], struggle with fine-grained visual perception [19, 69], and often hallucinate details [41, 84, 98, 105]. To address these challenges, we introduce a large-scale VQA dataset to enhance fine-grained visual understanding in VLMs along with a benchmark suite to evaluate this capability.

VLM Training Data. While most proprietary VLMs rely on closed-source training data [1, 4, 13, 63, 80], recent efforts have prioritized open-data alternatives. Molmo [15] introduced an open-data model competitive with proprietary systems, while SmolVLM [50] and PerceptionLM [10] scale this paradigm using diverse datasets spanning captioning [2, 44, 62, 103, 106], grounding [31, 36, 66, 85, 110], spatial reasoning [19, 30, 45], math [3, 12, 47], and chart-/diagram understanding [32, 54, 61, 79, 95]. Most relevant to us are SpotTheDiff [29] and Birds-to-Words [18], which pair images with text describing differences. In contrast, TWIN is more comprehensive and larger in size: TWIN features both matching and non-matching pairs, enabling reasoning about sameness and difference, distinctions in TWIN are finer and pertain to subtle cues, TWIN is far larger (561K pairs vs. 13K of SpotTheDiff and 3.3K of Birds-to-Words), and it spans diverse object types beyond a single domain such as birds. A detailed comparison is in the Appendix.

Fine-grained Recognition categorizes images into specific subgroups [96], with applications in classifying plants [58, 87, 88], birds [86, 92], vehicles [35, 49] and recently, retail products [6, 9, 22, 33]. These tasks are typically framed as 1-of-N classification or retrieval, making them ill-suited for evaluating VLMs. We repurpose popular benchmarks [33, 88, 91, 97, 107] and design a task to evaluate the fine-grained VQA abilities of VLMs.

VLM Post-training. Post-training refines VLMs by instilling specialized capabilities and aligning them with human intent. Supervised fine-tuning (SFT) [42, 56, 109] and distillation [25, 71, 102] transfer task-specific skills from annotated data or teacher models, but often cause forgetting and reduced generalization [11, 75]. Reinforcement learning mitigates these issues, advancing instruction-following [64, 68, 104], reasoning [13, 21, 46, 99, 104], and spatial understanding [17, 52, 72]. Beyond post-training methodology, the choice of data plays a critical role in driving post-training success. We demonstrate that reinforcement learning on our fine-grained TWIN dataset increases the perceptual precision of VLMs while preserving their performance on core image–language tasks.

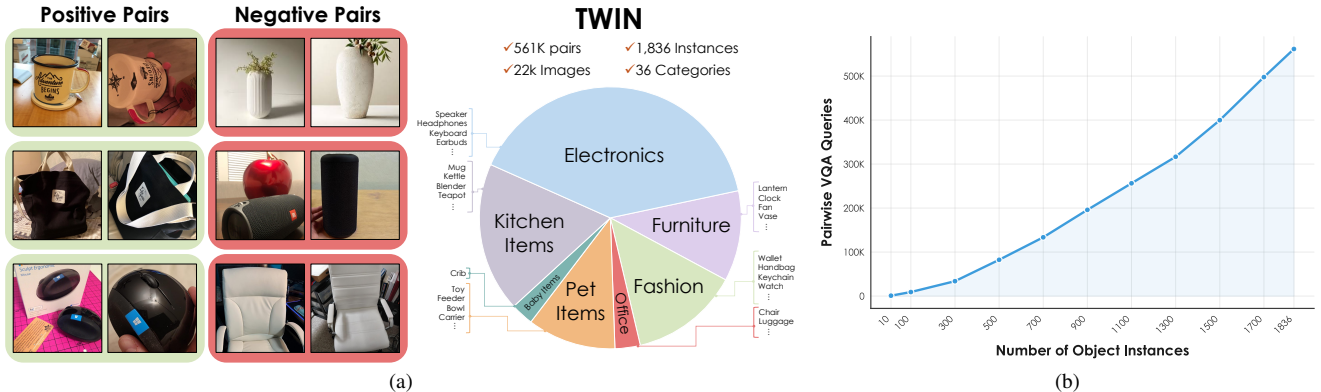


Figure 2. (a) TWIN is a large-scale VQA dataset for fine-grained visual understanding, where VLMs determine whether two images depict the same instance. TWIN contains 561K pairwise VQA queries across 1, 836 object instances, spanning 36 categories of common objects and over 22K images. (b) Scalability of the pairwise construction: from 1, 836 instances, TWIN yields 561K pairwise queries.

3. The TWIN Dataset

We present TWIN, a large-scale VQA dataset for advancing fine-grained visual understanding in VLMs. Existing training corpora emphasize broad visual understanding – spatial relations, common knowledge, and category-level recognition – offering little supervision for fine perception. As shown in Fig. 1(a), current VLMs often miss subtle cues essential for reliable perception. To address this, TWIN introduces 561,000 instance-centric queries where models are tasked to judge whether two similar looking images depict the same object instance. This design rewards attention to nuanced, instance-level details such as shape, texture, and part geometry, going beyond category-level understanding. Fig. 2 shows samples from TWIN and its statistics.

3.1. Dataset Construction

Task Definition. In our task, fine-grained visual understanding requires distinguishing object instances – recognizing when two images show the same object rather than the same category. We define an instance as a set of images of the same physical object under varied viewpoints, lighting, and backgrounds, consistent with prior work [33, 59, 60, 97, 107]. From this definition, we design a VQA task where a VLM receives two images and determines if they depict the same instance. Unlike category-level recognition (*e.g.*, cat vs dog), our task demands sensitivity to fine, instance-specific cues – shape, texture, and part geometry – that distinguish similar objects. Fig. 1(a) shows the setup; VQA prompts are in the Appendix.

Sourcing Instances. We source object instances across diverse categories from Amazon Reviews [24]. For each object instance, we collect images with varied contexts, viewpoints, and lighting to ensure visual diversity. Human annotators verify that each image clearly shows and identifies the object. We generate positive pairs by sampling from images

of the same instance. Fig. 2a shows examples of positive pairs along with the dataset’s distribution.

Hard Negative Pairs. A balanced dataset for fine-grained understanding requires both positive and negative pairs. If all examples were positive, the task would be trivial. Likewise, random negatives are often too easy (*e.g.*, a mug paired with a fan). We therefore focus on hard negatives – distinct objects that appear similar. We collect these hard negatives with the help of human annotators. First, using CLIP [67], we compute pairwise cosine similarities between image embeddings to shortlist visually similar candidates, from which human annotators select the final pairs. Examples of such hard negative pairs are shown in Fig. 2a, including two white vases with slightly different shapes and two white chairs differing in texture and armrest design.

Generated Negatives. Collecting hard negatives is costly and difficult to scale, so we augment TWIN with synthetic negatives using personalized image generation, DreamBooth [70]. Given images of an instance, DreamBooth produces similar variants that retain overall appearance but alter fine details, simulating hard negatives without extra data collection. The rightmost speaker in Fig. 2a demonstrates this: its color and geometry match the left one, but it omits the red logo and lighter contours. Each synthetic image is verified by human annotators. Details on image generation and additional examples are in the Appendix. We validate the impact of these generated negatives in our experiments.

Dataset Statistics. TWIN features 561K pairwise VQA queries, with 123K positive and 438K negative samples, spanning 22,157 unique images of 1,836 object instances, with 5,288 generated images. We plot the number of pairwise queries vs the number of object instances in Fig. 2b, highlighting the scalability of our pairwise formulation: TWIN’s size scales favorably with the number of object instances. Our scaling analysis in Sec. 5.2 demonstrates that collecting TWIN at scale is crucial for performance.



Figure 3. **FGVQA** is a suite of fine-grained VQA benchmarks spanning retail products (TWIN, ILIAS [33]); animals and plants (INQUIRE [88]); LANDMARKS [97]; birds (CUB [91]); and art (MET [107]). We include two query types: *pair* (top row), where a VLM judges if two images depict the same instance, species, or landmark, and *multi* where it counts how many images match a reference.



Figure 4. **Training VLMs on TWIN.** We train VLMs using RL on TWIN. Reward is computed by comparing the predicted answer with the ground truth pair assignment.

3.2. Training VLMs on TWIN

To improve fine-grained understanding in VLMs and evaluate the impact of our new dataset, we post-train existing models on TWIN. Our task requires recognizing subtle attributes to distinguish similar instances, and we hypothesize that optimizing for this task enhances broader fine-grained abilities. We post-train with RL as it is shown to improve model capabilities while preserving prior skills [11, 26, 40, 75]. Fig. 4 outlines our model training approach.

Setup. Given image pairs (I_1, I_2) with ground truth label $y \in \{\text{yes}, \text{no}\}$, a VLM π_θ , parametrized by θ , is prompted to produce a textual explanation and a final answer \hat{y} whether both images depict the same instance. We use a binary outcome reward comparing prediction and ground truth: $R(y, \hat{y}) = \mathbf{1}_{\{y=\hat{y}\}}$. Importantly, supervision relies *only* on pairwise assignments, without any descriptive textual annotations.

Optimization. We tune our VLM π_θ using GRPO [73] as it balances maximizing expected advantages while preventing drift from the pre-trained VLM. Details are in the Appendix.

Implementation. We train Qwen2.5-VL-3B-Instruct [5] and InternVL3.5-1B-Instruct [94] on TWIN, chosen as leading open-source VLMs at the 3B and 1B scales. Training is end-to-end on 4 A100 GPUs for 1 epoch with a batch size of 480, group size 5, and learning rate 10^{-6} . We use verl [76] for optimization and balance positive and negative queries in each batch. Hyperparameters are in the Appendix.

4. The FGVQA Benchmark Suite

Despite their strong general visual abilities, current VLMs struggle with fine-grained understanding [69, 89]. Existing VQA benchmarks emphasize broad image understanding, leaving this capability largely unevaluated. To this end, we introduce FGVQA, a suite of fine-grained VQA benchmarks that measure how well VLMs identify subtle visual cues. We show examples in Fig. 3 and provide more details below.

Benchmarks. Fine-grained understanding is a general skill – models attuned to subtle differences should generalize across domains. To evaluate this, we repurpose recognition and retrieval datasets, totaling 12,000 queries spanning diverse domains: MET [107] (artworks such as paintings and sculptures), ILIAS [33] (retail products), LANDMARKS [97] (monuments), CUB [91] (bird species), INQUIRE [88] (animals and plants from iNaturalist [87]), and TWIN-Eval, collected like TWIN but with unseen instances. The breadth of FGVQA enables assessment of cross-domain generalization.

Query types. For FGVQA, we construct two query types per dataset. *Pair* queries show two images and ask whether they depict the same instance, artwork, or species. *Multi* queries provide a reference image and three candidates, and ask how many match the reference. Each dataset includes 1,000 balanced examples per type: pair queries split evenly among positive and negative cases, while multi queries distribute uniformly across answer counts (250 each from 0-3). Examples are shown in Fig. 3, Fig. 5, and the Appendix.

Applicability. FGVQA provides a general framework for evaluating fine-grained recognition in VLMs. First, it probes visual perception – testing whether models can distinguish subtle differences that support accurate reasoning. Second, the pairwise yes/no format aligns with recognition and retrieval tasks, since both 1-of-N classification and retrieval can be cast as a sequence of pairwise comparisons. Together, these properties make FGVQA a practical, domain-general suite for analyzing perception in VLMs.

	MEAN	Pair	TWIN-Eval		ILIAS [33]		LANDMARKS [97]			MET [107]			CUB [91]		INQUIRE [88]				
			Multi	Total	Pair	Multi	Total	Pair	Multi	Total	Pair	Multi	Total	Pair	Multi	Total			
<i>Proprietary VLMs</i>																			
GPT4o [1]	86.1	92.2	71.2	81.7	95.0	95.5	95.3	87.3	74.7	81.0	86.3	72.9	79.6	91.7	86.0	88.9	94.3	86.3	90.3
Gemini 2.5 Flash [13]	82.2	89.1	68.1	78.6	92.2	90.5	91.4	85.4	77.0	81.2	82.6	71.9	77.3	84.1	77.9	81.0	88.3	79.4	83.9
<i>Open-Source VLMs</i>																			
PerceptionLM 3B [10]	37.8	46.9	25.2	36.1	49.6	25.0	37.3	51.5	25.7	38.6	50.4	26.1	38.3	49.6	24.9	37.3	52.1	26.1	39.1
Moondream 2 2B [55]	45.9	64.5	30.0	47.3	58.7	30.3	44.5	59.8	25.2	42.5	84.3	27.0	55.7	50.6	43.3	47.0	51.9	25.1	38.5
Gemma3 4B [82]	68.7	68.1	39.5	53.8	88.4	46.5	67.5	91.2	55.2	73.2	87.9	57.5	72.7	91.2	55.2	73.2	90.0	48.7	69.4
SmolVLM2 2.2B [50]	46.9	54.7	25.1	39.9	52.2	29.7	41.0	54.1	29.6	41.9	73.9	27.9	50.9	81.5	35.0	58.3	73.0	25.7	49.4
<i>Direct Comparisons</i>																			
Qwen2.5-VL 3B [5]	53.0	70.4	29.8	50.1	54.5	32.5	43.5	79.5	28.2	53.9	81.6	29.4	55.5	84.0	37.4	60.7	74.4	34.3	54.4
+ TWIN	67.0 _{+14.0}	88.9 _{+18.5}	45.7 _{+15.9}	67.3 _{+17.2}	79.9 _{+25.4}	43.7 _{+11.2}	61.8 _{+18.3}	80.8 _{+1.3}	34.9 _{+6.7}	57.9 _{+4.0}	85.4 _{+3.8}	46.5 _{+17.1}	66.0 _{+18.5}	92.5 _{+8.5}	57.7 _{+20.3}	75.1 _{+14.4}	92.7 _{+18.3}	54.6 _{+20.3}	73.7 _{+19.3}
InternVL3.5 1B [94]	51.3	67.2	25.9	46.6	60.0	39.1	49.6	54.1	33.5	43.8	73.9	47.1	60.5	56.1	40.5	48.3	80.4	37.9	59.2
+ TWIN	54.2 _{+2.9}	73.0 _{+5.8}	26.5 _{+0.6}	49.8 _{+3.2}	73.2 _{+13.2}	38.0 _{+1.1}	55.6 _{+6.0}	57.2 _{+3.1}	36.3 _{+2.8}	46.8 _{+3.0}	77.6 _{+3.7}	47.5 _{+0.4}	62.6 _{+2.1}	62.6 _{+6.5}	41.5 _{+1.0}	52.1 _{+3.8}	76.0 _{+4.4}	40.0 _{+2.1}	58.0 _{+1.2}

Table 1. **Accuracy (%) on FGVQA.** For *Pair* queries, VLMs are shown two images and asked if they show the same instance. On *multi* queries, VLMs are shown a reference image and three candidates and asked how many show the same instance as the reference. We report accuracy on each constituent dataset separately and the mean. Training on TWIN improves performance, even on domains not in TWIN.

5. Experiments

We conduct extensive experiments, both quantitative and qualitative, to evaluate the utility of TWIN as a training dataset and task for improving fine-grained understanding. Our goals are threefold: (1) establish baseline performance on FGVQA, our new fine-grained VQA benchmark suite that repurposes existing datasets, (2) assess if training on TWIN improves perception across domains, and (3) ablate the decisions made in our dataset construction and model training.

Baselines. We compare to the following models:

(1) *Proprietary VLMs:* We establish baseline performance on FGVQA for GPT4o [1] and Gemini 2.5 Flash [13].

(2) *Open-Source VLMs:* We report leading open-source models PerceptionLM-3B [10], Moondream2-2B [55], Gemma3-4B [82], and SmolVLM2-2.2B [50].

(3) *Direct Comparisons:* We fine-tune Qwen2.5-VL 3B Instruct [5] and InternVL3.5 1B Instruct [94] to evaluate the value of TWIN across architectures and scales. Each base model is compared to its trained variant, denoted “+ TWIN”.

5.1. Main Results

Tab. 1 shows results on FGVQA. Model variants trained on TWIN are evaluated zero-shot on all datasets except TWIN-Eval. All other models are evaluated zero-shot. All models are prompted without in-context examples. We summarize our findings below.

Training on TWIN improves fine-grained understanding. Our direct comparisons show substantial gains from training on TWIN. Qwen2.5-VL (3B) achieves strong improvements across datasets: +18.3% on ILIAS (43.5% to 61.8%) and +17.2% on TWIN-Eval (50.1% to 67.3%). InternVL3.5 (1B), despite being smaller and thus less expressive, still shows consistent gains from post-training on TWIN: +3.8% on CUB (48.3% to 52.1%) and +3.0% on LANDMARKS (43.8% to 46.8%). These consistent improvements across both models indicate that TWIN benefits VLMs of different scales and architectures. Importantly, we observe improvement on *multi* queries, which differ in structure from our training data, suggesting improved fine-

grained perception rather than task overfitting.

Improvements transfer to unseen domains. Training on TWIN, which features everyday household objects, improves performance even in domains absent from its training distribution. Substantial gains are observed on animal and plant species (INQUIRE & CUB), and for art and landmarks (MET & LANDMARKS), which are distinct from objects in TWIN. With Qwen2.5-VL, INQUIRE accuracy rises by +19.3% (54.4% to 73.7%), CUB by +14.4% (60.7% to 75.1%), and LANDMARKS by +4% (53.9% to 57.9%).

Qualitative Examples. We present qualitative results in Fig. 5, comparing baseline models with their counterparts post-trained on TWIN. The textual explanations reveal which visual cues models rely on, showing how TWIN enhances fine-grained reasoning. In (a), the trained Qwen2.5-VL distinguishes subtle color differences in the numbers and clock hands. In (c), it correctly identifies shared classical columns. In (e), it matches the reference card under challenging lighting in Image 2. In (g), the base model incorrectly flags Image 2 as a different knife, while the trained variant recognizes consistent blade texture and handle material. In (h), only the trained model notices color and design differences in the synthetic negative speaker (Image 3).

These improvements extend to out-of-distribution examples. In (b), the post-trained model identifies the bird by attending to its black head, white body, and orange beak. In (d), it notes differences in date and color scheme. In (f), it detects color differences between the reference bird and Image 3. These improved reasoning descriptions confirm that TWIN enhances understanding beyond the training domain.

Comparison to open-source VLMs. Among open-source baselines, Gemma3 performs best across benchmarks: 53.8% on TWIN-Eval, 69.4% on INQUIRE, and 72.7% on ILIAS. However, as Gemma3 does not support training with Flash Attention [14, 20, 28], fine-tuning it in PyTorch would be prohibitively expensive. Therefore, we train the second-best open-source VLM, Qwen2.5-VL, on TWIN. Our trained Qwen2.5-VL model (+ TWIN) outperforms Gemma3 on TWIN-Eval (67.3% vs 53.8%), INQUIRE (73.7% vs 69.4%), and CUB (75.1% vs 73.2%).



Figure 5. Outputs on FGVQA for base VLMs and variants trained on TWIN. For each example, we show the source dataset, images, and both model predictions. We include both pair queries (a-d) and multi queries (e-h). Incorrect reasoning is highlighted in red and correct reasoning in green. The red circle highlights a hard-to-see object. Training on TWIN enhances fine-grained grounding, leading to increased attention to part geometry and texture over the base model, even for domains that differ from the household objects in TWIN.

	MEAN	TWIN-Eval	ILIAS	LANDMARKS	MET	CUB	INQUIRE
Qwen2.5-VL 3B	53.0	50.1	43.5	53.9	55.5	60.7	54.4
+ TWIN w/o Hard Neg.	58.6	51.1	53.1	57.9	60.0	68.5	60.9
+ TWIN	63.1	65.3	58.4	54.9	64.4	66.9	68.7

Table 2. **Impact of hard negatives.** Models in rows 2 and 3 are trained on the TWIN variant of their corresponding row. The hard negatives in TWIN significantly improve performance on FGVQA.

Gemma3 outperforms our trained Qwen2.5-VL model on MET (72.7% vs 66.0%) and LANDMARKS (73.2% vs 57.9%) – the datasets where we see the least improvement from training.

Comparison to proprietary VLMs. We also benchmark proprietary models on FGVQA. GPT4o and Gemini-2.5-Flash outperform all open-source baselines (81.7% for GPT4o vs 53.8% for Gemma3 on TWIN-Eval; 91.4% for Gemini 2.5 Flash vs 67.5% for Gemma3 on ILIAS). These models are likely far larger and trained on proprietary data. Training on TWIN narrows this gap: Qwen2.5-VL + TWIN reaches 73.7% on INQUIRE, reducing the gap from 29.5% to 10.2%, showing that targeted fine-grained training substantially closes the gap with proprietary models.

5.2. Ablations and Analysis

We now analyze factors driving improved performance on FGVQA. First, we study the TWIN dataset and examining choices made during its construction, namely the challenging negative pairs (real and synthetic) in Tab. 2 and data scale in Fig. 6. Next, we compare post-training paradigms on TWIN, supervised fine-tuning vs reinforcement learning, in Tab. 3. Finally, we probe the vision encoder to showcase that training on TWIN improves underlying representations in Tab. 5. We summarize our findings below.

Hard Negatives. We evaluate the contribution of hard negatives to FGVQA performance in Tab. 2. We post-train Qwen2.5-VL 3B on two variants: (1) TWIN, a 250K-sample subset matching the original ratios of positive/negative and real/generated images—our final setting; and (2) TWIN w/o *Hard Neg.*, where all hard negatives are replaced with random negatives. This controlled comparison isolates the value of including hard negatives in TWIN. We report total accuracy (%) on each FGVQA dataset separately, as well as the mean across datasets.

Tab. 2 shows that even without hard negatives, our task yields modest improvements over the base model (51.1% vs 50.1% on TWIN-Eval; 60.0% vs 55.5% on MET). However, incorporating hard negatives improves performance by 4.5% on average (63.1% vs 58.6%). The gains are most pronounced on in-domain datasets like TWIN-Eval (65.3% vs 51.1%) and ILIAS (58.4% vs 53.1%), but remain substantial on out-of-distribution datasets like INQUIRE (68.7% vs 60.9%). These results validate our decision to collect human-verified hard negatives, demonstrating they are critical for developing fine-grained visual understanding.

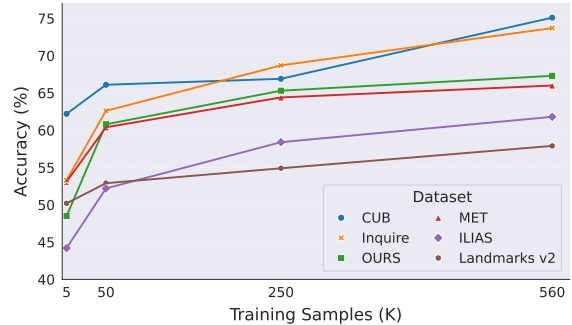


Figure 6. Effect of training set size on FGVQA accuracy (%).

	MEAN	TWIN-Eval	ILIAS	LANDMARKS	MET	CUB	INQUIRE
RL	57.5	64.0	50.3	48.5	58.7	65.0	58.7
SFT	53.8	61.2	53.6	47.6	52.3	53.9	54.2

Table 3. **SFT vs. RL.** We tune Qwen2.5-VL 3B on a subset of TWIN with SFT and RL. We report total accuracy (%) on FGVQA.

Scaling Analysis. Fig. 6 shows the impact of data scale for TWIN. We train a Qwen2.5-VL-Instruct 3B model with $M = \{5K, 50K, 250K, 561K\}$ image pairs and plot accuracy on FGVQA. We sample M with the same proportions of positive/negative pairs and real/generated images as our full dataset. Performance improves consistently across all datasets from 5K to 561K samples (e.g. 48.5% to 67.3% on TWIN and 44.2% to 61.8% on ILIAS), reinforcing our decision to collect TWIN at scale. Notably, scale also improves performance on domains not represented in TWIN: INQUIRE improves from 53.3% to 73.7% and CUB from 62.2% to 75.1% as training data scales from 5K to 561K.

SFT vs. RL. We compare post-training with reinforcement learning (RL) versus supervised fine-tuning (SFT) in Tab. 3. Our model produces both a chain-of-thought (CoT) explanation and a final yes/no prediction. RL optimizes a reward based solely on the final answer correctness, while SFT performs supervision on all output tokens, including both CoT and final prediction. To obtain high-quality supervision for SFT, we collect responses from Gemini-2.5-Flash [13] on a subset of TWIN and retain only those where Gemini is correct. We then post-train Qwen2.5-VL on these 136K pairs with both SFT and RL. Details for SFT are in the Appendix. Although both methods achieve similar performance on TWIN-Eval (61.2% with SFT vs 64.0% with RL), the RL variant outperforms on out-of-distribution datasets (53.9% with SFT vs 65.0% with RL on CUB; 52.3% with SFT vs. 58.7% with RL on MET). These results corroborate prior findings that RL better preserves generalization during post-training than SFT [11, 26, 40, 75].

Encoder Probing. We probe the underlying vision encoder of Qwen2.5-VL to examine whether training on TWIN improves its visual representations. Unlike contrastive models (e.g. CLIP [67]), this encoder was not trained to produce embeddings useful in isolation. Nevertheless, we apply traditional probing methods to assess representation quality

	REALWORLD [100]	POPE [41]	CV-BENCH [83]	NLVR2 [78]	AI2D [32]	SEED [39]	CHARTQA [54]	TEXTVQA [77]	BLINK [19]	MMMU [108]	VLM BIAS [89]
<i>Direct Comparisons</i>											
Qwen2.5 VL 3B [5]	59.8	87.6	66.0	79.8	78.6	75.0	83.4	79.4	47.3	47.1	17.2
+ TWIN	61.8	88.2	66.6	81.2	79.4	75.1	84.1	77.9	47.5	46.9	17.4
InternVL3.5 1B [94]	52.2	86.3	59.8	73.6	67.1	70.9	63.0	55.9	39.3	40.4	17.4
+ TWIN	52.6	86.3	60.2	73.8	67.2	70.8	63.2	55.7	39.7	40.1	17.4

Table 4. **Accuracy (%) on general VQA benchmarks.** VLMs post-trained on TWIN retain performance on general VQA benchmarks.

	PETS [65]		SUN397 [101]		CUB [91]		CIFAR100 [37]	
	Lin.	KNN	Lin.	KNN	Lin.	KNN	Lin.	KNN
Qwen2.5 VL 3B [5]	75.0	72.4	64.4	70.4	72.3	77.4	68.5	71.8
+ TWIN	79.1	74.5	66.4	71.8	72.4	77.7	69.6	73.2

Table 5. **Encoder probing results.** We evaluate Qwen2.5-VL’s vision encoder via linear probing and KNN. Post-training on TWIN yields embeddings better suited for fine-grained classification.

and determine if post-training on TWIN improves representation ability of vision encoders in VLMs. In Tab. 5, we report accuracy on fine-grained classification datasets covering various domains: PETS [65] with cat and dog species, SUN397 [101] with real world scenes, CUB [91] with bird species, and CIFAR100 [37] with everyday objects and animals. We follow [7] and evaluate two settings: a linear probe (Lin.) trained on embeddings from each dataset’s training split and then frozen for validation, and K-nearest neighbor retrieval (KNN), where test queries are matched against embeddings from the corresponding training split.

From Tab. 5, we find that post-training on TWIN yields consistent improvements across fine-grained classification datasets: +4.1% with a linear probe on PETS (75.0% to 79.1%), +1.4% with KNN on CIFAR100 (71.8% to 73.2%), and +2% with a linear probe on SUN397 (64.4% to 66.4%). The improvement to probing accuracy across datasets suggest that by forcing VLMs to detect subtle differences in objects, post-training on TWIN yields embeddings better suited for fine-grained understanding.

5.3. Additional Results

To ensure post-training on TWIN does not erode general visual reasoning, we report results on popular VQA benchmarks in Tab. 4. These benchmarks span common sense understanding (SEED [39], MMMU [108], NLVR2 [78]), spatial reasoning and grounding (REALWORLD [100], CV-BENCH [83], BLINK [19]), hallucination and bias (POPE [41], VLM BIAS [89]), OCR (TEXTVQA [77]), and chart/diagram understanding (CHARTQA [54], AI2D [32]). Although not our main focus, models post-trained on TWIN retain performance on general VQA benchmarks, with small improvements on most for both Qwen2.5-VL (+1.4% on NLVR2; +0.8% on AI2D) and InternVL3.5 (+0.4% on REALWORLD; +0.4% on CV-BENCH).

Beyond vision, Tab. 6 reports performance on popular text-only benchmarks covering different skills: MMLU [23] for common knowledge, HELLASWAG [111] for sentence completion, and GSM8K [12] for mathematical reasoning. We find that post-training leaves performance largely

	MMLU [23]	HELLASWAG [111]	GSM8K [12]
Qwen2.5 VL 3B [5]	64.7	66.4	70.8
+ TWIN	64.6	66.4	68.8
InternVL3.5 1B [94]	49.0	48.8	57.8
+ TWIN	49.0	48.9	58.1

Table 6. **Accuracy (%) on text-QA benchmarks.** Post-training on TWIN with RL leaves text-QA performance largely unaffected.

unchanged on these benchmarks: 64.7% vs 64.6% for Qwen2.5-VL on MMLU; 57.8% vs 58.1% for InternVL3.5 on GSM8K. These results reaffirm prior findings that RL-based tuning preserves model skills [11, 75].

6. Limitations & Future Work

We introduce TWIN, a large-scale VQA dataset of 561,000 queries designed for improving fine-grained perception in VLMs. Each query in TWIN asks whether two images depict the same object instance, forcing VLMs to perceive subtle visual cues to answer correctly. TWIN includes human-verified hard negative pairs, which we determine are crucial in our experiments. To measure progress on fine-grained understanding, we additionally introduce FGVQA, a benchmark suite for precise visual understanding across a wide range of domains. Current open-source VLMs struggle on FGVQA, but post-training them on TWIN substantially improves fine-grained reasoning, even on unseen domains. Our scaling analysis shows that collecting TWIN at scale is key for improved performance. We include a thorough failure analysis of post-trained models in the Appendix. There is an extensive list of future work to consider:

- We explore GRPO post-training with rewards applied only on final answers. More structured rewards, *e.g.* using multi-modal verifiers, may provide a richer learning signal and lead to improved perception capabilities.
- Our experiments show hard negatives in TWIN are essential for effective learning. Exploring automated techniques to mine even harder negatives, *e.g.* with the help of model-in-the-loop data engines, is a promising direction.
- TWIN includes substantial viewpoint variation, requiring models to reason over fine-grained part geometries that may appear different across image pairs. Integrating 3D representations as an explicit means of encoding spatial structure may further improve performance on the task.

We envision TWIN as a drop-in addition to VLM training corpora and hope FGVQA serves as a benchmark suite for measuring progress in fine-grained understanding. **To support future research in this direction, we will release all data, code, and post-trained models.**

Acknowledgments

We thank Aadarsh Sahoo, Ilona Demler, and Ziqi Ma for their feedback on the project. The project is funded by Meta through the LLM evaluation research grant and partly through Caltech’s CAST program. We also thank Google’s Gemma Academic program for granting us API credits for their LLMs.

References

- [1] Josh Achiam, Steven Adler, Sandhini Agarwal, Lama Ahmad, Ilge Akkaya, Florencia Leoni Aleman, Diogo Almeida, Janko Altenschmidt, Sam Altman, Shyamal Anadkat, et al. Gpt-4 technical report. *arXiv preprint arXiv:2303.08774*, 2023. [2](#), [5](#)
- [2] Harsh Agrawal, Karan Desai, Yufei Wang, Xinlei Chen, Rishabh Jain, Mark Johnson, Dhruv Batra, Devi Parikh, Stefan Lee, and Peter Anderson. Nocaps: Novel object captioning at scale. In *ICCV*, 2019. [2](#)
- [3] Aida Amini, Saadia Gabriel, Shanchuan Lin, Rik Koncel-Kedziorski, Yejin Choi, and Hannaneh Hajishirzi. Mathqa: Towards interpretable math word problem solving with operation-based formalisms. In *Proceedings of the 2019 Conference of the North American Chapter of the Association for Computational Linguistics: Human Language Technologies*, 2019. [2](#)
- [4] Anthropic. Claude, 2024. [2](#)
- [5] Shuai Bai, Keqin Chen, Xuejing Liu, Jialin Wang, Wenbin Ge, Sibo Song, Kai Dang, Peng Wang, Shijie Wang, Jun Tang, et al. Qwen2. 5-vl technical report. *arXiv preprint arXiv:2502.13923*, 2025. [1](#), [4](#), [5](#), [8](#)
- [6] Yalong Bai, Yuxiang Chen, Wei Yu, Linfang Wang, and Wei Zhang. Products-10k: A large-scale product recognition dataset. *arXiv preprint arXiv:2008.10545*, 2020. [2](#)
- [7] Daniel Bolya, Po-Yao Huang, Peize Sun, Jang Hyun Cho, Andrea Madotto, Chen Wei, Tengyu Ma, Jiale Zhi, Jathushan Rajasegaran, Hanoona Rasheed, et al. Perception encoder: The best visual embeddings are not at the output of the network. *arXiv preprint arXiv:2504.13181*, 2025. [8](#)
- [8] Ruojin Cai, Joseph Tung, Qianqian Wang, Hadar Averbuch-Elor, Bharath Hariharan, and Noah Snavely. Doppel-gangers: Learning to disambiguate images of similar structures. In *Proceedings of the IEEE/CVF International Conference on Computer Vision*, pages 34–44, 2023. [5](#)
- [9] Lele Cheng, Xiangzeng Zhou, Liming Zhao, Dangwei Li, Hong Shang, Yun Zheng, Pan Pan, and Yinghui Xu. Weakly supervised learning with side information for noisy labeled images. In *ECCV*, 2020. [2](#)
- [10] Jang Hyun Cho, Andrea Madotto, Effrosyni Mavroudi, Triantafyllos Afouras, Tushar Nagarajan, Muhammad Maaz, Yale Song, Tengyu Ma, Shuming Hu, Suyog Jain, et al. Perceptionlm: Open-access data and models for detailed visual understanding. *arXiv preprint arXiv:2504.13180*, 2025. [2](#), [5](#)
- [11] Tianzhe Chu, Yuexiang Zhai, Jihan Yang, Shengbang Tong, Saining Xie, Dale Schuurmans, Quoc V Le, Sergey Levine, and Yi Ma. Sft memorizes, rl generalizes: A comparative study of foundation model post-training. In *ICML*, 2025. [2](#), [4](#), [7](#), [8](#)
- [12] Karl Cobbe, Vineet Kosaraju, Mohammad Bavarian, Mark Chen, Heewoo Jun, Lukasz Kaiser, Matthias Plappert, Jerry Tworek, Jacob Hilton, Reiichiro Nakano, et al. Training verifiers to solve math word problems. *arXiv preprint arXiv:2110.14168*, 2021. [2](#), [8](#)
- [13] Gheorghe Comanici, Eric Bieber, Mike Schaekermann, Ice Pasupat, Naveen Sachdeva, Inderjit Dhillon, Marcel Blisstein, Ori Ram, Dan Zhang, Evan Rosen, et al. Gemini 2.5: Pushing the frontier with advanced reasoning, multimodality, long context, and next generation agentic capabilities. *arXiv preprint arXiv:2507.06261*, 2025. [2](#), [5](#), [7](#)
- [14] Tri Dao. Flashattention-2: Faster attention with better parallelism and work partitioning. In *ICLR*, 2024. [5](#)
- [15] Matt Deitke, Christopher Clark, Sangho Lee, Rohun Tripathi, Yue Yang, Jae Sung Park, Mohammadreza Salehi, Niklas Muennighoff, Kyle Lo, Luca Soldaini, et al. Molmo and pixmo: Open weights and open data for state-of-the-art multimodal models. *arXiv preprint arXiv:2409.17146*, 2024. [2](#)
- [16] Abhimanyu Dubey, Abhinav Jauhri, Abhinav Pandey, Abhishek Kadian, Ahmad Al-Dahle, Aiesha Letman, Akhil Mathur, Alan Schelten, Amy Yang, Angela Fan, et al. The llama 3 herd of models. *arXiv e-prints*, pages arXiv–2407, 2024. [2](#)
- [17] Yue Fan, Xuehai He, Diji Yang, Kaizhi Zheng, Ching-Chen Kuo, Yuting Zheng, Sravana Jyothi Narayanaraju, Xinze Guan, and Xin Eric Wang. Grit: Teaching mllms to think with images. In *NeurIPS*, 2025. [2](#)
- [18] Maxwell Forbes, Christine Kaeser-Chen, Piyush Sharma, and Serge Belongie. Neural naturalist: Generating fine-grained image comparisons. In *EMNLP*, 2019. [2](#), [5](#), [6](#), [7](#)
- [19] Xingyu Fu, Yushi Hu, Bangzheng Li, Yu Feng, Haoyu Wang, Xudong Lin, Dan Roth, Noah A Smith, Wei-Chiu Ma, and Ranjay Krishna. Blink: Multimodal large language models can see but not perceive. In *ECCV*, 2024. [1](#), [2](#), [8](#)
- [20] GitHub. Gemma3 github issue, 2025. [5](#)
- [21] Daya Guo, Dejian Yang, Haowei Zhang, Junxiao Song, Ruoyu Zhang, Runxin Xu, Qihao Zhu, Shirong Ma, Peiyi Wang, Xiao Bi, et al. Deepseek-r1: Incentivizing reasoning capability in llms via reinforcement learning. *arXiv preprint arXiv:2501.12948*, 2025. [2](#)
- [22] Sheng Guo, Weilin Huang, Xiao Zhang, Prasanna Srikhanta, Yin Cui, Yuan Li, Hartwig Adam, Matthew R Scott, and Serge Belongie. The imaterialist fashion attribute dataset. In *ICCV*, 2019. [2](#)
- [23] Dan Hendrycks, Collin Burns, Steven Basart, Andy Zou, Mantas Mazeika, Dawn Song, and Jacob Steinhardt. Measuring massive multitask language understanding. In *ICLR*, 2021. [8](#)
- [24] Yupeng Hou, Jiacheng Li, Zhankui He, An Yan, Xiusi Chen, and Julian McAuley. Bridging language and items for retrieval and recommendation. *arXiv preprint arXiv:2403.03952*, 2024. [3](#), [2](#)

- [25] Yushi Hu, Otilia Stretcu, Chun-Ta Lu, Krishnamurthy Viswanathan, Kenji Hata, Enming Luo, Ranjay Krishna, and Ariel Fuxman. Visual program distillation: Distilling tools and programmatic reasoning into vision-language models. In *CVPR*, 2024. 2
- [26] Maggie Huan, Yuetai Li, Tuney Zheng, Xiaoyu Xu, Seung-gone Kim, Minxin Du, Radha Poovendran, Graham Neubig, and Xiang Yue. Does math reasoning improve general llm capabilities? understanding transferability of llm reasoning. *arXiv preprint arXiv:2507.00432*, 2025. 4, 7
- [27] Drew A. Hudson and Christopher D. Mannin. Gqa: A new dataset for real-world visual reasoning and compositional question answering. In *CVPR*, 2019. 2
- [28] Huggingface. Gemma huggingface discussions, 2024. 5
- [29] Harsh Jhamtani and Taylor Berg-Kirkpatrick. Learning to describe differences between pairs of similar images. In *EMNLP*, 2018. 2, 5, 6, 7
- [30] Justin Johnson, Bharath Hariharan, Laurens Van Der Maaten, Li Fei-Fei, C Lawrence Zitnick, and Ross Girshick. Clevr: A diagnostic dataset for compositional language and elementary visual reasoning. In *CVPR*, 2017. 2
- [31] Sahar Kazemzadeh, Vicente Ordonez, Mark Matten, and Tamara Berg. Referitgame: Referring to objects in photographs of natural scenes. In *EMNLP*, 2014. 2
- [32] Aniruddha Kembhavi, Mike Salvato, Eric Kolve, Minjoon Seo, Hannaneh Hajishirzi, and Ali Farhadi. A diagram is worth a dozen images. In *ECCV*, 2016. 2, 8
- [33] Giorgos Kordopatis-Zilos, Vladan Stojnić, Anna Manko, Pavel Suma, Nikolaos-Antonios Ypsilantis, Nikos Efthymiadis, Zakaria Laskar, Jiri Matas, Ondrej Chum, and Giorgos Tolias. Ilias: Instance-level image retrieval at scale. In *CVPR*, 2025. 2, 3, 4, 5, 1, 8
- [34] Klemen Kotar, Stephen Tian, Hong-Xing Yu, Daniel LK Yamins, and Jiajun Wu. Are these the same apple? comparing images based on object intrinsics. In *NeurIPS*, 2023. 5
- [35] Jonathan Krause, Michael Stark, Jia Deng, and Li Fei-Fei. 3d object representations for fine-grained categorization. In *ICCVW*, 2013. 2
- [36] Ranjay Krishna, Yuke Zhu, Oliver Groth, Justin Johnson, Kenji Hata, Joshua Kravitz, Stephanie Chen, Yannis Kalantidis, Li-Jia Li, David A Shamma, et al. Visual genome: Connecting language and vision using crowdsourced dense image annotations. *International journal of computer vision*, 2017. 2
- [37] Alex Krizhevsky et al. Learning multiple layers of features from tiny images. 2009. 8
- [38] Kang-il Lee, Minbeom Kim, Seunghyun Yoon, Minsung Kim, Dongryeol Lee, Hyukhun Koh, and Kyomin Jung. Vlind-bench: Measuring language priors in large vision-language models. In *NAACL*, 2025. 1, 2
- [39] Bohao Li, Rui Wang, Guangzhi Wang, Yuying Ge, Yixiao Ge, and Ying Shan. Seed-bench: Benchmarking multi-modal llms with generative comprehension. *arXiv preprint arXiv:2307.16125*, 2023. 8
- [40] Tianle Li, Jihai Zhang, Yongming Rao, and Yu Cheng. Unveiling the compositional ability gap in vision-language reasoning model. *arXiv preprint arXiv:2505.19406*, 2025. 4, 7
- [41] Yifan Li, Yifan Du, Kun Zhou, Jinpeng Wang, Wayne Xin Zhao, and Ji-Rong Wen. Evaluating object hallucination in large vision-language models. In *EMNLP*, 2023. 2, 8
- [42] Zejun Li, Ruipu Luo, Jiwen Zhang, Minghui Qiu, Xuanjing Huang, and Zhongyu Wei. Vocot: Unleashing visually grounded multi-step reasoning in large multi-modal models. *arXiv preprint arXiv:2405.16919*, 2024. 2
- [43] Ji Lin, Hongxu Yin, Wei Ping, Pavlo Molchanov, Mohammad Shoeybi, and Song Han. Vila: On pre-training for visual language models. In *CVPR*, 2024. 2
- [44] Tsung-Yi Lin, Michael Maire, Serge Belongie, James Hays, Pietro Perona, Deva Ramanan, Piotr Dollár, and C Lawrence Zitnick. Microsoft coco: Common objects in context. In *ECCV*, 2014. 2
- [45] Fangyu Liu, Guy Edward Toh Emerson, and Nigel Collier. Visual spatial reasoning. *Transactions of the Association for Computational Linguistics*, 2023. 2
- [46] Zichen Liu, Changyu Chen, Wenjun Li, Penghui Qi, Tianyu Pang, Chao Du, Wee Sun Lee, and Min Lin. Understanding r1-zero-like training: A critical perspective. *arXiv preprint arXiv:2503.20783*, 2025. 2
- [47] Pan Lu, Ran Gong, Shibiao Jiang, Liang Qiu, Siyuan Huang, Xiaodan Liang, and Song-Chun Zhu. Inter-gps: Interpretable geometry problem solving with formal language and symbolic reasoning. In *ACL*, 2021. 2
- [48] Pan Lu, Hritik Bansal, Tony Xia, Jiacheng Liu, Chunyuan Li, Hannaneh Hajishirzi, Hao Cheng, Kai-Wei Chang, Michel Galley, and Jianfeng Gao. Mathvista: Evaluating mathematical reasoning of foundation models in visual contexts. In *ICLR*, 2024. 2
- [49] Subhansu Maji, Esa Rahtu, Juho Kannala, Matthew Blaschko, and Andrea Vedaldi. Fine-grained visual classification of aircraft. *arXiv preprint arXiv:1306.5151*, 2013. 2
- [50] Andrés Marafioti, Orr Zohar, Miquel Farré, Merve Noyan, Elie Bakouch, Pedro Cuenca, Cyril Zakka, Loubna Ben Allal, Anton Lozhkov, Nouamane Tazi, et al. Smolvlm: Redefining small and efficient multimodal models. *arXiv preprint arXiv:2504.05299*, 2025. 2, 5
- [51] Kenneth Marino, Mohammad Rastegari, Ali Farhadi, and Roozbeh Mottaghi. Ok-vqa: A visual question answering benchmark requiring external knowledge. In *CVPR*, 2019. 2
- [52] Damiano Marsili and Georgia Gkioxari. No labels, no problem: Training visual reasoners with multimodal verifiers. *arXiv preprint arXiv:2512.08889*, 2025. 2
- [53] Damiano Marsili, Rohun Agrawal, Yisong Yue, and Georgia Gkioxari. Visual agentic ai for spatial reasoning with a dynamic api. In *Proceedings of the Computer Vision and Pattern Recognition Conference*, pages 19446–19455, 2025. 2
- [54] Ahmed Masry, Xuan Long Do, Jia Qing Tan, Shafiq Joty, and Enamul Hoque. Chartqa: A benchmark for question

- answering about charts with visual and logical reasoning. In *ACL*, 2022. 2, 8
- [55] Moondream. moondream2, 2025. 2, 5
- [56] Niklas Muennighoff, Zitong Yang, Weijia Shi, Xiang Lisa Li, Li Fei-Fei, Hannaneh Hajishirzi, Luke Zettlemoyer, Percy Liang, Emmanuel Candès, and Tatsunori Hashimoto. s1: Simple test-time scaling. *arXiv preprint arXiv:2501.19393*, 2025. 2
- [57] Hyeon-Woo Nam, Ye-Bin Moon, Wonseok Choi, Hyun Lee, and Tae-Hyun Oh. Vlm’s eye examination: Instruct and inspect visual competency of vision language models. *Transactions on Machine Learning Research*, 2025, 2025. 5
- [58] Maria-Elena Nilsback and Andrew Zisserman. Automated flower classification over a large number of classes. In *2008 Sixth Indian conference on computer vision, graphics & image processing*. IEEE, 2008. 2
- [59] David Nister and Henrik Stewenius. Scalable recognition with a vocabulary tree. In *CVPR*, 2006. 3
- [60] Hyeonwoo Noh, Andre Araujo, Jack Sim, Tobias Weyand, and Bohyung Han. Large-scale image retrieval with attentive deep local features. In *ICCV*, 2017. 3
- [61] Jason Obeid and Enamul Hoque. Chart-to-text: Generating natural language descriptions for charts by adapting the transformer model. In *International Conference on Natural Language Generation*, 2020. 2
- [62] Yasumasa Onoe, Sunayana Rane, Zachary Berger, Yonatan Bitton, Jaemin Cho, Roopal Garg, Alexander Ku, Zarana Parekh, Jordi Pont-Tuset, Garrett Tanzer, et al. Docci: Descriptions of connected and contrasting images. In *ECCV*, 2024. 2
- [63] OpenAI. gpt-5, 2025. 2
- [64] Long Ouyang, Jeffrey Wu, Xu Jiang, Diogo Almeida, Carroll Wainwright, Pamela Mishkin, Chong Zhang, Sandhini Agarwal, Katarina Slama, Alex Ray, et al. Training language models to follow instructions with human feedback. 2022. 2
- [65] Omkar M Parkhi, Andrea Vedaldi, Andrew Zisserman, and CV Jawahar. Cats and dogs. In *CVPR*, 2012. 8
- [66] Bryan A Plummer, Liwei Wang, Chris M Cervantes, Juan C Caicedo, Julia Hockenmaier, and Svetlana Lazebnik. Flickr30k entities: Collecting region-to-phrase correspondences for richer image-to-sentence models. In *ICCV*, 2015. 2
- [67] Alec Radford, Jong Wook Kim, Chris Hallacy, Aditya Ramesh, Gabriel Goh, Sandhini Agarwal, Girish Sastry, Amanda Askell, Pamela Mishkin, Jack Clark, et al. Learning transferable visual models from natural language supervision. In *ICML*, 2021. 3, 7
- [68] Rafael Rafailov, Archit Sharma, Eric Mitchell, Stefano Ermon, Christopher D Manning, and Chelsea Finn. Direct preference optimization: your language model is secretly a reward model. In *NeurIPS*, 2023. 2
- [69] Pooyan Rahmazadehgervi, Logan Bolton, Mohammad Reza Taesiri, and Anh Totti Nguyen. Vision language models are blind: Failing to translate detailed visual features into words. *arXiv preprint arXiv:2407.06581*, 2024. 1, 2, 4
- [70] Nataniel Ruiz, Yuanzhen Li, Varun Jampani, Yael Pritch, Michael Rubinstein, and Kfir Aberman. Dreambooth: Fine tuning text-to-image diffusion models for subject-driven generation. In *CVPR*, 2023. 3, 4
- [71] Gabriel Sarch, Lawrence Jang, Michael Tarr, William W Cohen, Kenneth Marino, and Katerina Fragkiadaki. Vlm agents generate their own memories: Distilling experience into embodied programs of thought. *NeurIPS*, 2024. 2
- [72] Gabriel Sarch, Snigdha Saha, Naitik Khandelwal, Ayush Jain, Michael J Tarr, Aviral Kumar, and Katerina Fragkiadaki. Grounded reinforcement learning for visual reasoning. In *NeurIPS*, 2025. 2
- [73] Zhihong Shao, Peiyi Wang, Qihao Zhu, Runxin Xu, Junxiao Song, Xiao Bi, Haowei Zhang, Mingchuan Zhang, YK Li, et al. Deepseekmath: Pushing the limits of mathematical reasoning in open language models. *arXiv preprint arXiv:2402.03300*, 2024. 4, 3
- [74] Pratyusha Sharma, Tamar Rott Shaham, Manel Baradad, Stephanie Fu, Adrian Rodriguez-Munoz, Shivam Duggal, Phillip Isola, and Antonio Torralba. A vision check-up for language models. In *CVPR*, 2024. 1, 2
- [75] Idan Shenfeld, Jyothish Pari, and Pulkit Agrawal. RL’s razor: Why online reinforcement learning forgets less. *arXiv preprint arXiv:2509.04259*, 2025. 2, 4, 7, 8
- [76] Guangming Sheng, Chi Zhang, Zilingfeng Ye, Xibin Wu, Wang Zhang, Ru Zhang, Yanghua Peng, Haibin Lin, and Chuan Wu. Hybridflow: A flexible and efficient rlhf framework. In *Proceedings of the Twentieth European Conference on Computer Systems*, 2025. 4, 5
- [77] Amanpreet Singh, Vivek Natarajan, Meet Shah, Yu Jiang, Xinlei Chen, Dhruv Batra, Devi Parikh, and Marcus Rohrbach. Towards vqa models that can read. In *CVPR*, 2019. 8
- [78] Alane Suhr, Stephanie Zhou, Ally Zhang, Iris Zhang, Huanjun Bai, and Yoav Artzi. A corpus for reasoning about natural language grounded in photographs. In *Annual Meeting of the Association for Computational Linguistics*, 2019. 8
- [79] Benny J Tang, Angie Boggust, and Arvind Satyanarayan. Vistext: A benchmark for semantically rich chart captioning. In *ACL*, 2023. 2
- [80] Gemini Team, Rohan Anil, Sebastian Borgeaud, Jean-Baptiste Alayrac, Jiahui Yu, Radu Soricut, Johan Schalkwyk, Andrew M Dai, Anja Hauth, Katie Millican, et al. Gemini: a family of highly capable multimodal models. *arXiv preprint arXiv:2312.11805*, 2023. 2
- [81] Gemma Team, Thomas Mesnard, Cassidy Hardin, Robert Dadashi, Surya Bhupatiraju, Shreya Pathak, Laurent Sifre, Morgane Rivière, Mihir Sanjay Kale, Juliette Love, et al. Gemma: Open models based on gemini research and technology. *arXiv preprint arXiv:2403.08295*, 2024. 2
- [82] Gemma Team, Aishwarya Kamath, Johan Ferret, Shreya Pathak, Nino Vieillard, Ramona Merhej, Sarah Perrin, Tatiana Matejovicova, Alexandre Ramé, Morgane Rivière, et al. Gemma 3 technical report. *arXiv preprint arXiv:2503.19786*, 2025. 5
- [83] Shengbang Tong, Ellis Brown, Penghao Wu, Sanghyun Woo, Manoj Middepogu, Sai Charitha Akula, Jihan Yang,

- Shusheng Yang, Adithya Iyer, Xichen Pan, et al. Cambrian-1: A fully open, vision-centric exploration of multimodal llms. *NeurIPS*, 2024. 2, 8
- [84] Shengbang Tong, Zhuang Liu, Yuexiang Zhai, Yi Ma, Yann LeCun, and Saining Xie. Eyes wide shut? exploring the visual shortcomings of multimodal llms. In *CVPR*, 2024. 2
- [85] Jack Urbanek, Florian Bordes, Pietro Astolfi, Mary Williamson, Vasu Sharma, and Adriana Romero-Soriano. A picture is worth more than 77 text tokens: Evaluating clip-style models on dense captions. In *CVPR*, 2024. 2
- [86] Grant Van Horn, Steve Branson, Ryan Farrell, Scott Haber, Jessie Barry, Panos Ipeirotis, Pietro Perona, and Serge Belongie. Building a bird recognition app and large scale dataset with citizen scientists: The fine print in fine-grained dataset collection. In *CVPR*, 2015. 2
- [87] Grant Van Horn, Oisín Mac Aodha, Yang Song, Yin Cui, Chen Sun, Alex Shepard, Hartwig Adam, Pietro Perona, and Serge Belongie. The inaturalist species classification and detection dataset. In *CVPR*, 2018. 2, 4, 1
- [88] Edward Vendrow, Omiros Pantazis, Alexander Shepard, Gabriel Brostow, Kate E Jones, Oisín Mac Aodha, Sara Beery, and Grant Van Horn. Inquire: a natural world text-to-image retrieval benchmark. In *NeurIPS*, 2024. 2, 4, 5, 1, 8
- [89] An Vo, Khai-Nguyen Nguyen, Mohammad Reza Taesiri, Vy Tuong Dang, Anh Totti Nguyen, and Daeyoung Kim. Vision language models are biased. *arXiv preprint arXiv:2505.23941*, 2025. 1, 2, 4, 8
- [90] An Vo, Mohammad Reza Taesiri, Daeyoung Kim, and Anh Totti Nguyen. B-score: Detecting biases in large language models using response history. In *ICML*, 2025. 1, 2
- [91] Catherine Wah, Steve Branson, Peter Welinder, Pietro Perona, and Serge Belongie. The caltech-ucsd birds-200-2011 dataset. 2011. 2, 4, 5, 8, 1
- [92] Catherine Wah, Steve Branson, Peter Welinder, Pietro Perona, and Serge Belongie. The caltech-ucsd birds-200-2011 dataset. 2011. 2
- [93] Ke Wang, Junting Pan, Weikang Shi, Zimu Lu, Houxing Ren, Aojun Zhou, Mingjie Zhan, and Hongsheng Li. Measuring multimodal mathematical reasoning with math-vision dataset. *NeurIPS*, 37:95095–95169, 2024. 2
- [94] Weiyun Wang, Zhangwei Gao, Lixin Gu, Hengjun Pu, Long Cui, Xingguang Wei, Zhaoyang Liu, Linglin Jing, Shenglong Ye, Jie Shao, et al. Internvl3. 5: Advancing open-source multimodal models in versatility, reasoning, and efficiency. *arXiv preprint arXiv:2508.18265*, 2025. 4, 5, 8
- [95] Zirui Wang, Mengzhou Xia, Luxi He, Howard Chen, Yitao Liu, Richard Zhu, Kaiqu Liang, Xindi Wu, Haotian Liu, Sadhika Malladi, et al. Charxiv: Charting gaps in realistic chart understanding in multimodal llms. In *NeurIPS*. 2
- [96] Xiu-Shen Wei, Yi-Zhe Song, Oisín Mac Aodha, Jianxin Wu, Yuxin Peng, Jinhui Tang, Jian Yang, and Serge Belongie. Fine-grained image analysis with deep learning: A survey. *TPAMI*, 2021. 2
- [97] Tobias Weyand, Andre Araujo, Bingyi Cao, and Jack Sim. Google landmarks dataset v2-a large-scale benchmark for instance-level recognition and retrieval. In *CVPR*, 2020. 2, 3, 4, 5, 1, 8
- [98] Xiyang Wu, Tianrui Guan, Dianqi Li, Shuaiyi Huang, Xiaoyu Liu, Xijun Wang, Ruiqi Xian, Abhinav Shrivastava, Furong Huang, Jordan Boyd-Graber, et al. Autohallucination: Automatic generation of hallucination benchmarks for vision-language models. In *EMNLP*, 2024. 2
- [99] Zhiyu Wu, Xiaokang Chen, Zizheng Pan, Xingchao Liu, Wen Liu, Damai Dai, Huazuo Gao, Yiyang Ma, Chengyue Wu, Bingxuan Wang, et al. Deepseek-v12: Mixture-of-experts vision-language models for advanced multimodal understanding. *arXiv preprint arXiv:2412.10302*, 2024. 2
- [100] xAI. Real world qa, 2024. 8
- [101] Jianxiong Xiao, James Hays, Krista A Ehinger, Aude Oliva, and Antonio Torralba. Sun database: Large-scale scene recognition from abbey to zoo. In *CVPR*, 2010. 8
- [102] Guowei Xu, Peng Jin, Ziang Wu, Hao Li, Yibing Song, Lichao Sun, and Li Yuan. Llava-cot: Let vision language models reason step-by-step. In *ICCV*, 2025. 2
- [103] Hu Xu, Po-Yao Huang, Xiaoqing Tan, Ching-Feng Yeh, Jacob Kahn, Christine Jou, Gargi Ghosh, Omer Levy, Luke Zettlemoyer, Wen-tau Yih, et al. Altogether: Image captioning via re-aligning alt-text. In *Conference on Empirical Methods in Natural Language Processing*, 2024. 2
- [104] An Yang, Anfeng Li, Baosong Yang, Beichen Zhang, Binyuan Hui, Bo Zheng, Bowen Yu, Chang Gao, Chengen Huang, Chenxu Lv, et al. Qwen3 technical report. *arXiv preprint arXiv:2505.09388*, 2025. 2
- [105] Moon Ye-Bin, Nam Hyeon-Woo, Wonseok Choi, and Tae-Hyun Oh. Beaf: Observing before-after changes to evaluate hallucination in vision-language models. In *ECCV*, 2024. 2
- [106] Peter Young, Alice Lai, Micah Hodosh, and Julia Hockenmaier. From image descriptions to visual denotations: New similarity metrics for semantic inference over event descriptions. *Transactions of the association for computational linguistics*, 2014. 2
- [107] Nikolaos-Antonios Ypsilantis, Noa Garcia, Guangxing Han, Sarah Ibrahim, Nanne van Noord, and Giorgos Tolias. The met dataset: Instance-level recognition for artworks. In *NeurIPS*, 2021. 2, 3, 4, 5, 1, 8
- [108] Xiang Yue, Yuansheng Ni, Kai Zhang, Tianyu Zheng, Ruoqi Liu, Ge Zhang, Samuel Stevens, Dongfu Jiang, Weiming Ren, Yuxuan Sun, et al. Mmmu: A massive multi-discipline multimodal understanding and reasoning benchmark for expert agi. In *CVPR*, 2024. 2, 8
- [109] Eric Zelikman, Yuhuai Wu, Jesse Mu, and Noah Goodman. Star: Bootstrapping reasoning with reasoning. In *NeurIPS*, 2022. 2
- [110] Rowan Zellers, Yonatan Bisk, Ali Farhadi, and Yejin Choi. From recognition to cognition: Visual commonsense reasoning. In *CVPR*, 2019. 2
- [111] Rowan Zellers, Ari Holtzman, Yonatan Bisk, Ali Farhadi, and Yejin Choi. Hellaswag: Can a machine really finish your sentence? In *ACL*, 2019. 8
- [112] Renrui Zhang, Dongzhi Jiang, Yichi Zhang, Haokun Lin, Ziyu Guo, Pengshuo Qiu, Aojun Zhou, Pan Lu, Kai-Wei Chang, Yu Qiao, et al. Mathverse: Does your multi-modal

llm truly see the diagrams in visual math problems? In *ECCV*. Springer, 2024. [2](#)

- [113] Yaowei Zheng, Richong Zhang, Junhao Zhang, Yanhan Ye, Zheyang Luo, Zhangchi Feng, and Yongqiang Ma. Llamafactory: Unified efficient fine-tuning of 100+ language models. In *ACL*, 2024. [5](#)

Same or Not? Enhancing Visual Perception in Vision-Language Models

Supplementary Material

Contents

A Additional details on FGVQA	1
A.1 Evaluation Benchmarks	1
A.2 FGVQA Prompts	1
A.3 FGVQA Human Evaluation	1
B Additional details on TWIN	2
B.1 Instance Sourcing	2
B.2 De-Duplication	3
B.3 Hard Negative Pair Assignment	3
B.4 Additional Details on Generated Negatives	3
C Additional Training Details	3
C.1 GRPO	3
C.2 Supervised Fine-Tuning	5
D Failure Cases	5
E Additional Evaluations	5
E.1. Additional Benchmarks	5
E.2. In-Context Learning	5
F. Comparisons to Prior Datasets	5
F.1. Birds-To-Words	7
F.2. Comparison to SpotTheDiff	7

A. Additional details on FGVQA

We provide additional details on FGVQA, our new benchmark suite for evaluating fine-grained VQA. We describe the datasets included in FGVQA in Sec. A.1. We illustrate additional examples in Fig. 7, and describe all prompts used in Sec. A.2. We report exact match accuracy for all benchmarks on both *pair* and *multi* queries.

A.1. Evaluation Benchmarks

We describe the provenance of each benchmark in FGVQA below.

TWIN-Eval is the evaluation set of TWIN. It is collected identically to TWIN (Sec. 3), but features distinct instances and images from TWIN.

ILIAS [33] is a large-scale test dataset of instance-level image retrieval. It predominantly features images of retail products taken in various contexts, backgrounds, and lighting. For both *pair* and *multi* queries, we source images from the `core_db` split, using the `__key__` field to determine instance identity.

	MEAN	TWIN-Eval	ILIAS	LANDMARKS	MET	CUB	INQUIRE
Human	92.9	90.0	100.0	82.5	93.8	92.5	98.8

Table 7. Human Evaluations on FGVQA.

Google Landmarks v2 (LANDMARKS) [97] is a landmark recognition dataset featuring human-made and natural landmarks. The dataset has been used in both classification and retrieval settings. To ensure sufficient images per landmark to for *multi* queries, we source images from the `train` split and use the `label` field to determine landmark identity.

MET [107] is an image retrieval dataset featuring artwork from the Metropolitan Museum of Art in New York. The dataset features images of the same art piece or sculpture from varying viewpoints, emphasizing multi-view consistency in retrieval. We use the `mini_met` set to construct both *pair* and *multi* queries.

CUB [91] is a fine-grained classification dataset that focuses on identifying bird species from images. We use the `test` split for all queries and create *pair* and *multi* queries based on the specie of bird.

Inquire [88] is a benchmark for natural world image retrieval, featuring images of animal and plant species sourced from iNaturalist [87]. We source images from the `validation` split and use the `inat24_species_name` field to determine instance identity for both *pair* and *multi* queries.

A.2. FGVQA Prompts

We include all prompts used on all datasets for both *pair* and *multi* queries in Figs. 12 to 17. All prompts are identical in format, except for the domain-specific instance names (*e.g.* bird/object/artwork/species). Additionally, for benchmarks featuring object instances (TWIN-Eval, ILIAS [33]), we found it necessary to provide the definition of an object instance as models were incorrectly labeling different objects of the same-category (*e.g.* two earbuds of different colors) as the same.

A.3. FGVQA Human Evaluation

We establish human performance on FGVQA in Tab. 7. We task four human annotators with repsonding to a subset of 20 queries per benchmark in FGVQA. We report total accuracy (%) on each dataset, averaged across evaluator. We find that human evaluators significantly outperform open-source VLMs, suggesting ample future work is needed in fine-grained VQA.

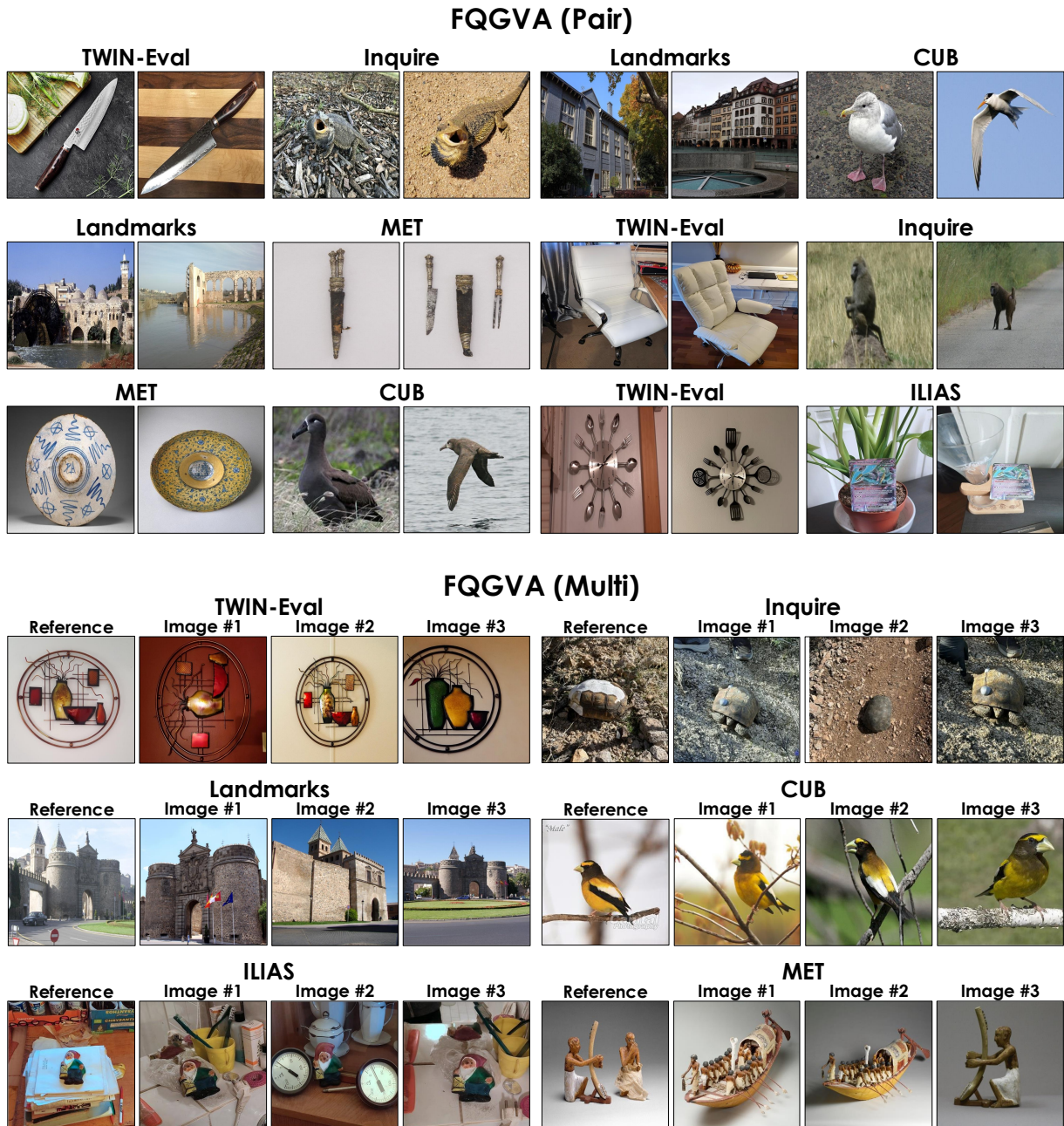


Figure 7. **Additional examples from FGVQA.** We show examples of images in *pair* and *multi* queries. FGVQA spans six datasets across a wide range of domains, creating a challenging suite for assessing cross-domain fine-grained VQA in VLMs.

B. Additional details on TWIN

We provide further details on the collection of TWIN, including instance sourcing, de-duplication, hard negative pair assignment, and details on generating synthetic negatives.

B.1. Instance Sourcing

We used the Amazon Reviews dataset [24] to extract a large set of product listings, which would serve as candidate objects, and associated noisy review images. We categorized these objects into supercategories based on their associated category in the Amazon store (*e.g.* “Electronics”) and further into categories based on the product title (*e.g.* “Speaker”). We aimed to maximize diversity in

our instances and thus selected 36 categories to draw from. We subsequently tasked human annotators with removing products that either lacked visual consistency (*e.g.* the same product being sold in multiple colors) or did not adhere to the object category (*e.g.* “earbud replacement tips” instead of “earbuds”).

B.2. De-Duplication

To ensure the correctness of the pairwise labels in TWIN, we must ensure that object instances are *unique*. If object instances are not unique, then two of the same objects could incorrectly be listed as negative pairs. However, on Amazon duplicate listings are common. We therefore merged duplicate objects into the same instance. To this end, we used a pre-trained CLIP model to compare the images of each product with the images of all other products via cosine similarity. We flagged the k images with the highest similarity as potential duplicates, setting k equal to the number of images for the product. We then tasked human annotators with manually inspecting the flagged images. If a duplicate was found, we merged the two products. The resulting object instances after de-duplication are used to produce the 561K instances of TWIN.

B.3. Hard Negative Pair Assignment

Once we have collected a set of object instances, we construct hard negative pairs – pairs of distinct objects that appear similar. We collect these hard negatives with the help of human annotators. First, using CLIP [67], for each object instance, we compute pairwise cosine similarities between the image embeddings of that instance and all other instances. We use these similarities to shortlist k visually similar candidates for each instance, with k being a random number between $1 - 2 \times$ the number of positive images of that instance. Human annotators then select the final pairs, omitting pairs they deem to be too easy.

B.4. Additional Details on Generated Negatives

We augment the set of negative pairs with additional synthetically generated images. Augmenting with generated negatives allows us to produce additional negative pairs without extra data collection. We follow the procedure outlined in Dreambooth [70]. For each object instance, we sample 3 to 5 images for each instance to serve as grounding images. We set the initializer tokens to the generic category associated with the instance (*e.g.* “vase”, “headphones”). Our prompts to Dreambooth are: [“an image of {category}”, “similar to {category}”, “a picture of {category}”, “show me a {category}”, “here is a {category}”] replacing {category} with the category of the instance. Finally, we task human annotators with validating the generated samples. Annotators are asked to remove generations that either do not appear similar to the instance

or are indistinguishable from the instance – yielding a set of hard negative pairs.

We show additional examples of synthetic negative pairs in Fig. 8. For each pair of images, we show the real image on the left and the paired synthetic image on the right. We find that synthetic negatives faithfully capture the “gist” and overall appearance of the object instance, but they fail to capture nuanced details such as part color and geometry, texture, and brand text/logos. These subtle differences in appearances yield an augmenting set of hard negative pairs.

C. Additional Training Details

We include additional details for all model training. In Sec. C.1, we provide an overview of GRPO [73], our main post-training method, and our training setup. We provide additional details on supervised fine-tuning (Sec. 5.2) in Sec. C.2. We include all hyperparameters in Tab. 10 and Tab. 11.

C.1. GRPO

To post-train VLMs on TWIN, we use Group Relative Policy Optimization (GRPO; [73]). We provide an overview of this method below.

Setup. Given a pair of images (I_1, I_2) with ground-truth pairwise label $y \in \{\text{yes}, \text{no}\}$, our base VLM π_θ , parametrized by θ , is prompted to produce a reasoning explanation r and final answer \hat{y} whether both images depict the same instance. We wish to find π_{θ^*} that correctly identifies pairs of images that show the same instance. We include the VQA prompt used during training in Fig. 18.

Reward Design. We define a simple binary outcome reward R that compares the predicted final answer with the ground truth pairwise assignment: $R(y, \hat{y}) = \mathbf{1}_{\{y=\hat{y}\}}$. Our supervision thus relies *only* on pairwise assignments and does not use any descriptive textual annotations.

Optimization. We optimize our VLM π_θ via GRPO [73]. For each image pair (I_1, I_2) with ground truth label y , we sample G responses: $\mathcal{O} = \{(I_1, I_2, r^{(i)}, \hat{y}^{(i)})\}_{i=1}^G$ and compute centralized advantages:

$$A^{(i)} = R(y, \hat{y}^{(i)}) - \frac{1}{G} \sum_{j=1}^G R(y, \hat{y}^{(j)}) \quad (1)$$

The GRPO objective then directly maximizes expected advantages while maintaining policy stability:

$$\begin{aligned} \mathcal{L}(\theta) &= \frac{1}{G} \sum_{i=1}^G \left(\hat{A}^{(i)} - \beta \text{KL}[\pi_\theta \parallel \pi_{\text{ref}}] \right) \\ \hat{A}^{(i)} &= \min \left(s^{(i)} A^{(i)}, \text{clip}(s^{(i)}, 1 - \epsilon, 1 + \epsilon) A^{(i)} \right) \end{aligned} \quad (2)$$

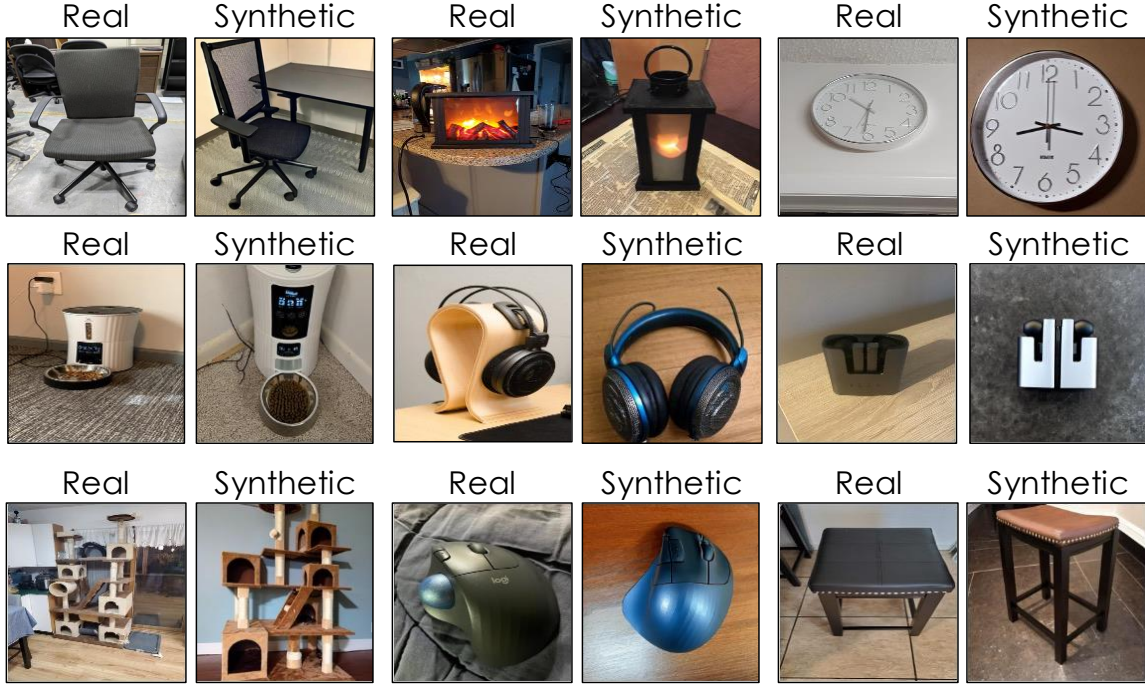


Figure 8. **Additional Synthetic Negatives.** For each pair, we show a real image of the object instance and a synthetic image of the same instance generated with Dreambooth [70]. We find the synthetic negatives capture the “gist” of the instance, but are not faithful to fine details such as color, geometry, and texture – making them a strong additional set of hard negative pairs.

(a) Landmarks

InternVL 3.5 (TWIN)

These two images depict **different landmarks**. The first image shows a **well-preserved stone castle** with a clear blue sky, while the second image shows a **more dilapidated and partially ruined stone structure** with a dirt path and scattered vegetation. **The first image likely represents a historical or ancient castle, whereas the second image appears to be a ruin or a less preserved structure, possibly from a different time period or location.**

Answer: no ❌

(b) MET

InternVL 3.5 (TWIN)

Both images depict a similar figure, but **there are some differences in the details and posture**. The first image shows the figure from a frontal perspective, while the second image shows it from a rear perspective. The figure in the first image is standing upright with arms slightly raised, whereas the figure in the second image is standing with one leg forward and the other bent, **with arms hanging by the sides.**

Answer: no ❌

(c) CUB

Qwen2.5-VL (TWIN)

The first image shows a bird with a long, pointed beak and dark plumage, which is characteristic of a cormorant. The second image also depicts a **bird with a similar appearance**, including a long beak and dark plumage, which is consistent with the characteristics of a cormorant. Based on the visual similarities in beak shape and plumage coloration, it is reasonable to conclude that **these two birds are likely the same species, specifically a cormorant.**

Answer: yes ❌

(d) ILIAS

InternVL 3.5 (TWIN)

The first image shows a collection of books on a shelf, including one titled “EX 4th Edition” by Herbert Voss. The second image shows a glass with a small blue creature inside it, which appears to be a **Squirtle from the Pokémon series**. These images do not contain the same or identical products. The first image is a collection of books, while the second image is a glass containing a toy. The content and nature of the items are different, making them distinct products.

Answer: no ❌

(e) INQUIRE

Qwen2.5-VL(TWIN)

Both images depict a hippopotamus. The first image shows a hippopotamus in its natural habitat, partially submerged in water, which is typical behavior for this species. The second image also shows a hippopotamus, but it appears to be in a different environment, possibly a forested area, which is consistent with the known habitats of hippos. The presence of the animal’s distinctive features such as the large body, thick skin, and the way it moves through the water supports the identification of both images as depicting the same species.

Answer: yes ❌

(f) TWIN-Eval

Qwen2.5-VL (TWIN)

The two images show the same product, which is an Invicta watch. 1) Brand and Model: Both images display an Invicta watch. 2) Watch Face: The watch face in both images has a similar design with a white background, gold accents, and a chronograph function. 3) Branding: The brand name “INVICTA” is visible on the watch face in both images. 4) Box and packaging: Both watches are presented in yellow boxes with white inserts. Given that all these characteristics match between the two images, it can be concluded that they are **indeed the same product.**

Answer: yes ❌

Figure 9. **Failure Cases on FGVQA for models post-trained on TWIN.** For each example, we show the source dataset, images, and model predictions. Incorrect reasoning is highlighted in red. The red circle highlights hard-to-see objects.

where $s^{(i)} = \frac{\pi_{\theta}(r^{(i)}, \hat{y}^{(i)} | I_1, I_2)}{\pi_{\text{old}}(r^{(i)}, \hat{y}^{(i)} | I_1, I_2)}$ represents the importance ratio, $\epsilon = 0.2$ is the clipping parameter, and $\beta = 0.01$

is the KL penalty coefficient. The formulation encourages improved fine-grained understanding while simultaneously

preventing drift from the pre-trained base policy π_{ref} .

Implementation. We train Qwen2.5-VL-3B-Instruct [5] and InternVL3.5-1B-Instruct [94] on TWIN, chosen as leading open-source VLMs at the 3B and 1B scales. We do not freeze any part of the model, and train on 4 A100 GPUs for 1 epoch. We use a batch size of 480, group size 5 and learning rate 10^{-6} . We build on the verl [76] repository for training. We detail all hyperparameters in Tab. 10. Post-training the Qwen2.5-VL 3B model for one epoch on the 560K samples of TWIN took approximately 140 hours on 4 A100 GPUs.

C.2. Supervised Fine-Tuning

We compare post-training methods in Sec. 5.2. We provide additional details for supervised fine-tuning (SFT) used in those experiments. As our model produces both an explanation and final prediction, SFT requires supervision beyond the pairwise assignment labels used in RL. To obtain high-quality supervision, we prompt Gemini-2.5-Flash [13] with samples from TWIN and retain responses where Gemini is correct. We use default generation parameters for Gemini and collect a total of 136K high-quality answers.

We train Qwen2.5-VL 3B end-to-end using SFT on the collected samples. We use LLaMa-Factory [113] for training, using a learning rate of 10^{-6} with a cosine scheduler. We train the SFT model for 2 epochs, as this yielded better accuracy on FGVQA. All hyperparameters are in Tab. 11.

D. Failure Cases

We include failure cases for models post-trained with TWIN in Fig. 9. For each example, we show the source dataset, images, and model predictions. We find that although models post-trained with TWIN demonstrate improved fine-grained understanding, they struggle with fine differences in color (*e.g.* in (a) where the ruins appears different colors due to lighting, and (f) where the watch accents differ between blue and gold). Moreover, extreme viewpoint variation, as seen in (b) remains a challenge. Lastly, we find that models struggle to extrapolate from incomplete views of the animals in (c) and (e). These challenging examples additionally highlight the difficulty of our new FGVQA benchmark suite.

InternVL on Inquire. We observe a slight decrease in performance on INQUIRE (-1.2%) when post-training InternVL3.5 1B on TWIN. We investigate the model responses and find that post-training the 1B model on TWIN reduces “direct identification” (*e.g.*, naming a species) and emphasizes comparisons of visual cues (*e.g.*, the color of the feathers). While this improves instance-level reasoning, it can fail under challenging lighting or occlusion, where the base model succeeds by relying more on priors.

E. Additional Evaluations

We provide additional evaluations for models post-trained with TWIN. In Sec. E.1 we explore the impact of post-training on TWIN on the related tasks of monument doppelganger detection and evaluate sensitivity to color and shapes. In Sec. E.2 we compare post-training to prompting with in-context-learning examples.

E.1. Additional Benchmarks

We evaluate on an additional set of benchmarks to determine if post-training on TWIN improves robustness to other image variations. We compare the baseline Qwen2.5-VL 3B model with our TWIN post-trained variant on monument doppelganger detection [8], the “yes or no” queries on shape/color sensitivity from VLMs Eye [57], and 500 pairwise queries from CUTE [34] in Tab. 8.

	Doppel. [8]	Shape Sens. [57]	Color Sens. [57]	CUTE [34]
Qwen2.5-VL 3B	50.8	56.8	96.1	58.8
+ TWIN	55.2	95.7	99.7	68.0

Table 8. **Additional benchmarks.**

Post-training on TWIN improves doppelganger detection (+4.4%), despite TWIN not including monuments. This mirrors the gains on LANDMARKS and MET seen in Tab. 1. Similarly, post-trained models improve at detecting dissimilar shapes (+38.9%), reach near-perfect performance at comparing colors (99.7%) and are more robust to photometric variations (+9.2% on CUTE). These results reaffirm that TWIN pushes models to attend to subtle visual cues over coarse semantic similarity.

E.2. In-Context Learning

We report results on FGVQA for in-context-learning (+ICL) prompting in Sec. E.2 to explore if we can achieve improved performance via sophisticated prompting as opposed to post-training. We randomly sample one positive and one negative pair from TWIN as in-context examples for each FGVQA query.

	Mean	TWIN-Eval	ILIAS	Landmarks	MET	CUB	Inquire
Qwen2.5-VL 3B (+ ICL)	39.5	39.0	37.3	37.5	38.5	43.5	41.2
Qwen2.5-VL 3B (+ TWIN)	67.0	67.3	61.8	57.9	66.0	75.1	73.7

Table 9. **In-Context Learning.**

Post-training significantly outperforms in-context-learning (67.0% vs 39.5% on average). In the ICL setting, the 3B model appears to infrequently misunderstand the order of images in the prompt, or ignores the examples entirely.

F. Comparisons to Prior Datasets

We provide a more detailed comparison to prior datasets Birds-To-Words [18] and SpotTheDiff [29]. While both of these datasets also feature pairs of images as input (similar to TWIN), there are several key differences. First, the task in these datasets is to identify the differences between

Birds-to-Words

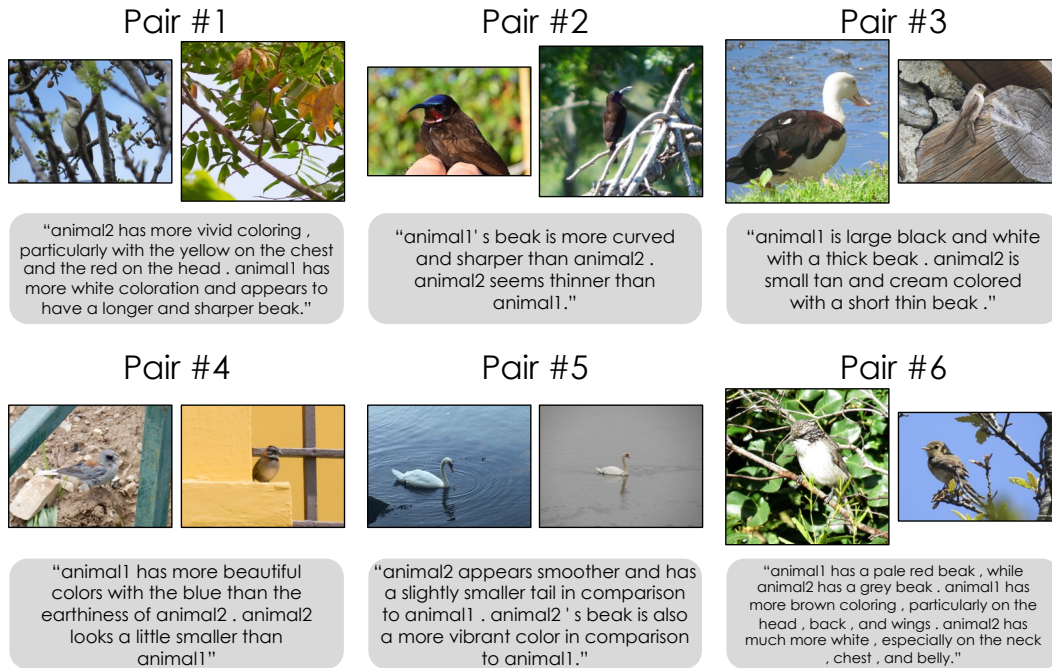


Figure 10. Examples from Birds-to-Words [18]. The dataset features 3.3K pairs of *different* bird species, along with a human-annotated description of their differences. The differences are often coarse-grained (e.g. Pair 3, Pair 6 – which both display significant color differences), and the text descriptions subjective (e.g. Pair 4 – where animal 1 is described as “more beautiful” than animal 2).

SpotTheDiff

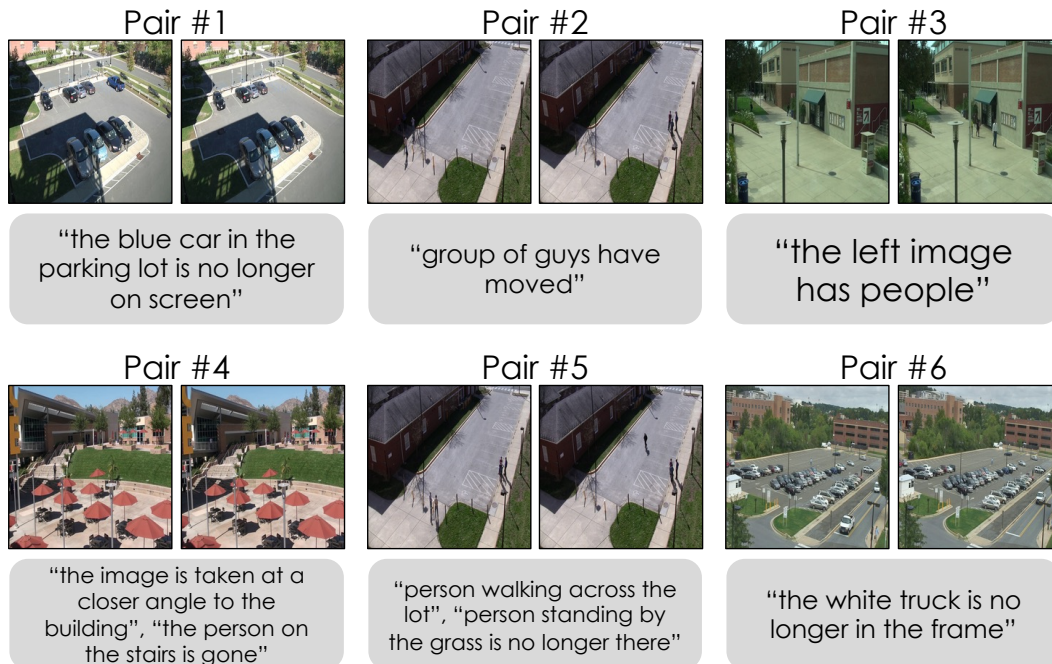


Figure 11. Examples from SpotTheDiff [29]. The dataset features 13K pairs of images taken from different frames of the same video. Unlike TWIN, that emphasizes fine differences in object texture and geometry, the differences in SpotTheDiff are primarily spatio-temporal (e.g. Pair 1 with the blue car leaving the frame, Pair 2 with the people moving) and highly coarse-grained (e.g. Pair 3).

two images, with the assumption *a priori* that the images are indeed different. In contrast, TWIN includes both negative pairs and positive pairs in which the instance is unchanged, requiring models to reason about both similarities and differences rather than only locating discrepancies. Second, the differences captured in TWIN are substantially more fine-grained, often involving subtle variations in texture or part geometry that go beyond the relatively coarse differences in prior datasets. Third, our dataset is considerably larger in scale (561K pairs vs. 13K for SpotTheDiff and 3.3K for Birds-To-Words). We provide examples and describe the differences with each individual dataset in more detail below.

F.1. Birds-To-Words

Birds-to-words [18] features 3.3K pairs of images of different bird species, along with human-annotated descriptions of the differences. We show examples from the dataset in Fig. 10. We observe that, unlike the fine-grained differences in TWIN, the differences are often much coarser (*e.g.* Pair 3 and Pair 6, which both feature significant color differences). Moreover, the human-annotated descriptions can be subjective (*e.g.* Pair 4 which describes one bird as “more beautiful”).

Compared to TWIN, the dataset is orders of magnitude smaller (3.3K pairs vs the 561K in TWIN) and spans only bird species, while TWIN features a wide range of object categories with significantly different geometries (*e.g.* earbuds and mugs). Additionally, Birds-to-Words features almost exclusively *negative* pairs. While a small number of pairs are annotated as depicting the same instance, these are anomalous cases and not a core aspect of the dataset – the task is fundamentally to describe the differences between two images. In contrast, TWIN emphasizes both positive and negative pairs, requiring models to recognize not only differences but also similarities.

F.2. Comparison to SpotTheDiff

SpotTheDiff [29] comprises 13K pairs of images sourced from two different frames of the same video. The videos used depict large scenes from security camera footage. As a result, the differences between frames are predominantly spatio-temporal, concerning which objects or people are visible or no longer visible in the scene (*e.g.* a car leaving the frame, a person moving positions). We visualize examples from SpotTheDiff [29] in Fig. 11. These examples highlight that differences are generally coarse-grained and, unlike the examples in TWIN, do not require reasoning about viewpoint variation, part-level geometry, or fine-grained texture changes. Similar to Birds-to-Words, SpotTheDiff assumes the paired images are different, whereas TWIN additionally emphasizes recognizing similarities through the inclusion of positive pairs. Finally,

TWIN is orders of magnitude larger in scale (561K vs. 13K pairs) and introduces challenges not present in SpotTheDiff, including substantial viewpoint variation, lighting changes, and differences in context and background.

Pair: Are these images of the same or identical products? For two products to be considered identical, minor changes such as those that can be explained context, backgrounds or photography conditions are allowed, but characteristic features of the product (color, shape, size, etc.) should remain consistent. For images with multiple products, compare only the primary product.
Explain your reasoning and then conclude with a yes or no answer in <answer> tags as <answer>yes</answer> or <answer>no</answer>.

Multi: The first image is a reference image. How many of the other images depict the same or identical products as the reference image? For two products to be considered identical, minor changes such as those that can be explained by context, backgrounds or photography conditions are allowed, but characteristic features of the product (color, shape, size, etc.) should remain consistent. For images with multiple products, compare only the primary product.
Explain your reasoning and then answer with a number from 0 to 3 in <answer> tags as <answer>n</answer>.

Figure 12. FGVQA Prompts: TWIN-Eval.

Pair: Do these images contain the same or identical products? For two products to be considered identical, minor changes such as those that can be explained by context, backgrounds or photography conditions are allowed, but characteristic features of the product (color, shape, size, etc.) should remain consistent.
Explain your reasoning and then answer with a yes or no answer in <answer> tags as <answer>yes</answer> or <answer>no</answer>.

Multi: The first image is a reference image. How many of the other images contain the same or identical products to one in the reference image? For two products to be considered identical, minor changes such as those that can be explained by context, backgrounds or photography conditions are allowed, but characteristic features of the product (color, shape, size, etc.) should remain consistent.
Explain your reasoning and then answer with a number from 0 to 3 in <answer> tags.

Figure 13. FGVQA Prompts: ILIAS [33].

Pair: Do these two images contain the same landmark?
Explain your reasoning then answer with a yes or no answer in <answer> tags as <answer>yes</answer> or <answer>no</answer>.

Multi: The first image is a reference image. How many of the other images contain the same landmark as the reference image?
Explain your reasoning then answer with a number from 0 to 3 in <answer> tags.

Figure 14. FGVQA Prompts: LANDMARKS [97].

Pair: Do these two images contain the same piece of art?
Explain your reasoning and then answer with a yes or no answer in <answer> tags as <answer>yes</answer> or <answer>no</answer>.

Multi: The first image is a reference image. How many of the other images contain the same piece of art as the reference image?
Explain your reasoning and then answer with a number from 0 to 3 in <answer> tags.

Figure 15. FGVQA Prompts: MET [107].

Pair: Do these two images show a bird of the same species?
Explain your reasoning and then conclude with a yes or no answer in <answer> tags as <answer>yes</answer> or <answer>no</answer>.

Multi: The first image is a reference image. How many of the other images show a bird of the same species as the reference image?
Explain your reasoning and then conclude with a number from 0 to 3 in <answer> tags.

Figure 16. FGVQA Prompts: CUB [91].

Pair: Do these two images show an animal or plant of the same scientific species?
Explain your reasoning and then answer with a yes or no answer in <answer> tags as <answer>yes</answer> or <answer>no</answer>.

Multi: The first image is a reference image. How many of the other images show an animal or plant of the same scientific species as the reference image?
Explain your reasoning and then answer with a number from 0 to 3 in <answer> tags.

Figure 17. FGVQA Prompts: INQUIRE [88].

Are these images of the same or identical products? For two products to be considered identical, minor changes such as those that can be explained by context, backgrounds or photography conditions are allowed, but characteristic features of the product (color, shape, size, etc.) should remain consistent. For images with multiple products, compare only the primary product. Explain your reasoning and then conclude with a yes or no answer in <answer> tags as <answer>yes</answer> or <answer>no</answer>.

Figure 18. Prompt used for training with TWIN.

Hyperparameter	Value
Batch size	480
Group size	5
Max prompt length	2048
Max response length	2048
Learning rate	1e-6
Optimizer	AdamW
Weight decay	0.01
KL coefficient	0.01
Clip ratio	0.2
Epochs	1
Rollout engine	vLLM
Temperature	1.0
Top-p	1.0
Gradient clipping	Max norm 1.0
Freeze vision tower	False
Mixed precision	bf16

Table 10. Hyperparameters for GRPO training.

Hyperparameter	Value
Batch size	256
Max prompt length	2048
Max response length	2048
Learning rate	1e-6
Optimizer	AdamW
Scheduler	Cosine
Warmup ratio	0.1
Epochs	2
Deepspeed config	ZeRO Stage 3
Gradient clipping	auto
Freeze vision tower	False
Mixed precision	bf16

Table 11. Hyperparameters for SFT training.